Technical Report
TR-15-04
August 2016

Comparative cation exchange capacity experiments on Laxemar fracture coating material using four different methods

Anna Neubeck

SVENSK KÄRNBRÄNSLEHANTERING AB

SWEDISH NUCLEAR FUEL
AND WASTE MANAGEMENT CO

Box 250, SE-101 24 Stockholm
Phone +46 8 459 84 00
skb.se

SVENSK KÄRNBRÄNSLEHANTERING

ISSN 1404-0344
SKB TR-15-04
ID 1470770

August 2016

Comparative cation exchange capacity experiments on Laxemar fracture coating material using four different methods

Anna Neubeck, Stockholm University

Keywords: Fracture coatings, Laboratory, Leaching, Cation Exchange Capacity (CEC).

Abstract

A series of leaching studies have been performed in which the cation exchange capacity (CEC) has been determined for fracture coating minerals from Äspö-Laxemar. Different batch and flow leaching experiment techniques have been compared.

The results indicate a strong heterogeneity among the analyzed samples and large differences between the different methods. The different sample sizes, mineralogical compositions as well as the chosen CEC method are suggested to be the main reasons for the differences in the results.

The relatively new method of cation exchange capacity determination using cobalt hexaammine was tested and shown to be most suitable for the fracture infills used in this study, as this method was not affected by calcite dissolution. The obtained CEC values with this method were below 52 meq/100 g (milli equivalents per 100 g of sample).

Sammanfattning

Lakstudier har utförts i vilka katjonbyteskapacitet (CEC) har bestämts för sprickfyllnadsmineral från Äspö-Laxemar. Flera typer av skak- och flödesexperimenttekniker har jämförts.

Resultaten tyder på en stark heterogenitet bland de analyserade proverna och stora skillnader mellan de olika metoderna. De olika provstorlekarna, mineralogiska sammansättningarna samt de valda CEC metoderna föreslås vara de viktigaste orsakerna till skillnaderna i resultaten.

Den relativt nya metoden för katjonbyteskapacitetsbestämning med användning av kobolt hexaammin testades och som visade sig vara den mest lämpliga metoden för den typen av sprickfyllnadsmaterial som använts i denna studie, eftersom denna metod inte påverkades av kalcitupplösning. De erhållna CEC värdena var med denna metod under 52 mekv/100 g (milliekvivalenter per 100 g prov).

Contents

1 Introduction 7

2 Experimental methods 9
2.1 Sampling 9
2.2 Cation Exchange Determinations 9
2.2.1 Desorption with flow-through experiments 9
2.2.2 Desorption experiments using standard $BaCl_2$-method 10
2.2.3 Desorption experiments using standard NH_4Ac-method 11
2.2.4 Desorption experiments using standard $Co(NH_3)_6^{3+}$-method 12
2.3 Analyses 12
2.3.1 Mineral characterisation 12
2.3.2 Analysis of liquid phases (ICP-OES) 13

3 Results and discussion 15
3.1 Solid characterization 15
3.1.1 SEM-EDS 15
3.1.2 B.E.T. 22
3.2 Cation-Exchange measurements 22
3.2.1 Flow-through experiments 22
3.2.2 $BaCl_2$ exchange 24
3.2.3 $Co(NH_3)_6Cl_3$ exchange 25
3.2.4 NH_4Ac 26

4 Discussion 29

5 Conclusions 33

6 Acknowledgements 35

References 37

Appendix 39

1 Introduction

Ion exchange in clay minerals is a process that affects substantially the compositions of groundwaters in granite fractures, i.e. the Na/Ca ratio, and the levels of K and Mg. It is therefore an important process to characterize when making long-term evaluations of the conditions around high- and low-level nuclear waste repositories. In addition, ion-exchange will also contribute to the retention of any radionuclides leaving the repository.

Many methods for determining the CEC (Cation Exchange Capacity) in soils and crystalline rocks have been developed for different types of materials (Skinner et al. 2002, Liu et al. 2001). Soils with a high content of calcite will inevitably result in an overestimation of the exchangeable Ca^{2+} ion content within the soil due to calcite dissolution (which is influenced by pH and/or degassing of CO_2, ion strength, etc) if the methods are not improved to avoid this dissolution. Byegård and Tullborg (2012) compared different CEC methods showing that the CEC standard method ISO 13536:1995 (using $BaCl_2$) does not seem to be suitable for fault gouge rock material <0.125 mm size fractions as they found indications of poor replacement of Ba^{2+} by Mg^{2+} ions in the second step. In the study by Byegård and Tullborg (2012) a new standard CEC method ISO 23470:2007 involving Co-hexaammine, resulted in a higher selectivity of the $Co(NH_3)_6^{3+}$ ion compared to the replacement of Mg^{2+} ions in the ISO 13536:1995 $BaCl_2$ method. Also, the $Co(NH_3)_6^{3+}$-method only involves a single step and will thus be less sensitive to uncertainty and contamination.

The present study aims to investigate the suitability of the $Co(NH_3)_6^{3+}$, $BaCl_2$ and NH_4Ac methods (Ross and Ketterings 2011, standards ISO 13536:1995 and ISO 23470:2007, respectively) for determining CEC of fracture coating material from Laxemar, SE Sweden. It also aims to investigate two additional methods: a flow-through method for CEC determination and the NH_4Ac method described in Byegård and Tullborg (2012).

2 Experimental methods

2.1 Sampling

Fracture coating samples from Äspö/Laxemar were collected in November 2012 from the drill core archive in Oskarshamn in consultation with Henrik Drake (Isochron Geoconsulting, Sweden). Sampling was focused to borehole sections with *a*) existing hydrochemical data and *b*) host rock composition representative for the Äspö/Laxemar area. The samples were chosen with as large as possible spreading in depths, in order to cover different ground water regimes and thus aqueous chemistry. The samples were chosen from *a*) shallow depths, *b*) repository depths (500 ± 50 m), and *c*) deeper than repository depth. Insofar it was possible, samples were collected from drill core sections in which groundwater has been sampled and chemically characterized at or close to the selected section.

The fracture coating material used in all experiments was extracted from fracture material found in drill cores without crushing or grinding of the material. Fracture coating material from boreholes KLX08, KLX09, KLX11A, KLX13A, KLX16A and KA1596A02 were used for the experiments, see Table 2-1. The dominating fracture mineral was chlorite in all samples followed by calcite and quartz, see Table 3-1 (Section 3.1). Most of the samples suffered of shortage of material, which may have increased the spreading of the results. The shortage of material also resulted in using material only from Laxemar and not Forsmark.

The material was prepared according to the international standard ISO 11464:2006, i.e. air dried at 40 °C prior to use and sieved to fraction sizes: *a*) 0–63 µm, *b*) 63–125 µm, *c*) 125–500 µm and *d*) 500 µm to 1 mm. No washing or liquid treatment was made on the samples due to a risk of a possible structural or compositional change of the material. Mineralogical descriptions of representative samples were made using X-Ray Diffraction (XRD) and Scanning Electron Microscopy – Electron Dispersive Spectrometry (SEM-EDS) and the results are presented in Section 3.1.1.

Table 2-1. List of samples collected for this study.

Drill core	Elevation (m.a.s.l.)	Drill core length (m)
KLX08	−165	218.54–218.75
KLX09	−691	720.15–720.30
KLX11A	−459	510.45–510.67
KLX13A	−466	494.37–494.84
	−503	531.98–532.66
	−550	578.03–578.56
KLX16A	−11	33.95–34.20
KA1596A02	−220	4.32–5.00

2.2 Cation Exchange Determinations

2.2.1 Desorption with flow-through experiments

This method consists of a flow-through multi-step procedure in which an aqueous solution (either deionized water or KCl solutions of different concentrations) is passed through the sample in a column connected to a peristaltic pump with a flow rate of 0.5 mL/min (Figure 2-1). KCl solutions are used in order to be able to compare the results from a pure water solution with those using a solution with higher ionic strength. Potassium ions were chosen in order to be able to analyze the sodium/calcium ratio. Liquid samples are collected continuously and the total amount of leached cations is measured after every experiment. This method monitors the time at which cations are desorbed from the sample.

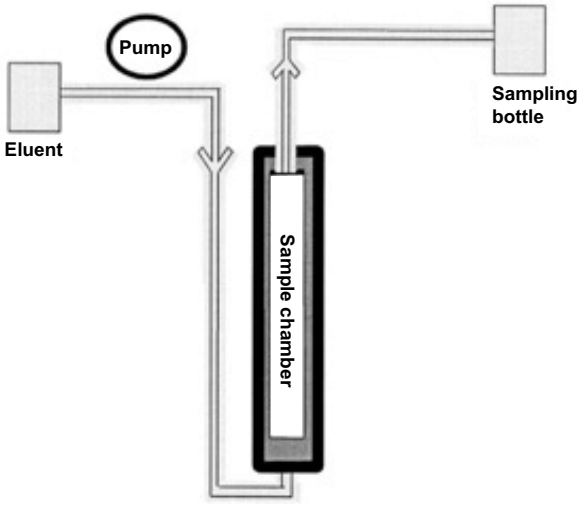

Figure 2-1. *Schematic drawing of the plug flow-reactor. From Frogner and Schweda (1998).*

Approximately 2 g of dried and sieved fracture coating material from boreholes KLX09, KLX13A and KLX16A were used, cf. Table 2-2. The fracture coating samples were placed between two filters inside a Teflon flow-through column (Figure 2-1) and fluids with various compositions (Milli-Q water, 0.001M KCl, 0.01M KCl and 0.02M KCl) were passed through the column with a flow rate of 0.5 mL/min. The collection of liquid samples was continuous and each liquid sample volume was 10 mL. The total collected sample volume was 120 mL and the total duration of the experiment was 130 min for each fracture coating sample. All liquid samples were passed through a 0.4 µm filter prior to analysis, and 10 µL of concentrated HNO_3 (puriss. Sigma Aldrich) was added to all samples prior to ICP analysis. The total charge concentration of the major cation elements is reported in meq/100 g sample. Blank samples were prepared by repeating the flow-through experiments, without any mineral sample.

Table 2-2. List of samples, sample drill core depth, grain size fractions and sample mass used in the flow-through experiments.

Drill cores	Drill core length (m)	Elevation (m.a.s.l.)	Grain size (µm)	Sample mass (g)	Flow-through solution
KLX09	720.15–720.30	−691	0–125	2.003	0.001 M KCl
KLX09	720.15–720.30	−691	0–125	1.547	0.01 M KCl
KLX09	720.15–720.30	−691	0–125	1.547	0.02 M KCl
KLX13A	494.37–494.84	−466	0–125	2.086	Deionized water
KLX13A	578.03–578.56	−503	0–125	2.588	Deionized water
KLX13A	494.37–494.84	−466	125–250	2.001	Deionized water
KLX13A	578.03–578.56	−503	125–250	2.007	Deionized water
KLX16A	33.95–34.20	−11	0–125	2.002	0.001 M KCl
KLX16A	33.95–34.20	−11	0–125	2.003	0.01 M KCl
KLX16A	33.95–34.20	−11	0–125	2.003	0.02 M KCl

2.2.2 Desorption experiments using standard $BaCl_2$-method

ISO 13536:1995 is a standard batch method for CEC determination in which two steps are included. All samples were first saturated with a $BaCl_2$ solution (1 mol/L) whereby the cation exchange sites on the sample material are saturated with Ba^{2+} ions. An excess of $MgSO_4$ (0.02 mol/L) is then added to the sample and the adsorbed Ba^{2+} ions are exchanged by Mg^{2+} ions. Leaching of Ba^{2+} is favoured by the addition of SO_4^{2-} to the solution, i.e. the leached Ba forms $BaSO_4$(s) which favours further Mg-Ba exchange. The amount of leached cations from the first exchange reaction should then equal the amount of exchanged Ba^{2+} ions (i.e. the decrease of Mg concentration) from the second treatment and the decrease in the Mg concentration should give the total CEC of the material.

Sample masses between 1.4–13.8 g of dried and sieved fracture coating minerals (Table 2-3) were used for the experiments. The samples were prepared according to the standard method ISO 13536:1995, with minor modifications. The standard method requires the use of a minimum sample mass of 10 g for samples low in humus and clays and 2.5 g for samples with high contents in clays. Since the collected sample sizes in some cases did not reach the required mass, a larger spreading and uncertainties can be expected for these sample sizes (Table 2-3).

Table 2-3. List of samples, sample drill core depth, grain size fractions and sample mass used in the $BaCl_2$ experiments.

Drill cores	Drill core length (m)	Elevation (m.a.s.l.)	Grain size (µm)	Sample mass (g)
KLX09	720.15–720.30	−691	0–63	1.45
KLX13A	578.03–578.56	−550	0–63	5.79
KA1596A02	4.32–5.00	−220	0–63	4.47
KLX13A	494.37–494.84	−466	63–125	13.79
KLX13A	531.98–532.66	−503	63–125	2.23
KLX13A	494.37–494.84	−466	250–500	5.01
KLX13A	578.03–578.56	−550	250–500	5.07
KLX13A	494.37–494.84	−466	500–1000	5.04
KLX13A	531.98–532.66	−503	500–1000	5.00
KLX13A	578.03–578.56	−550	500–1000	5.00

2.2.3 Desorption experiments using standard NH_4Ac-method

The ISO 13536:1995 involves saturation of sample with 1M NH_4Ac (pH ~ 7) to extract all cations from the sample. This is a single step method in which all exchanged cations should correspond to the cation exchange capacity of the material.

A modified (according to Byegård and Tullborg 2012) standard method NFX 31-130 was used for CEC determination of fracture coating samples from bore holes KLX04, KLX09, KLX11A, KLX13A and KA1596A02 (Table 2-4). Sample masses between 1.06–5.10 g of dried and sieved samples (Table 2-4) were used for the experiments. The variation of sample mass was due to shortage of material. All samples were prepared according to the standard method ISO 13536:1995: the samples were added to the NH_4Ac solution, shaken and allowed to stand overnight. Thereafter the fracture-coating minerals were filtered, the filtrate was diluted and analyzed for exchanged cations with ICP-OES (Inductively Coupled Plasma Optical Emission Spectrometry). Since the collected sample sizes in this study in some cases were far below the mass required (25 g) by the standard method, the results obtained in this study might have larger spreading and uncertainties

Table 2-4 List of samples, sample drill core depth, grain size fraction and sample mass used in the NH_4Ac-experiments.

Drill core	Drill core length (m)	Elevation (m.a.s.l.)	Grain size (µm)	Sample mass (g)
KLX13A	494.37–494.84	−466	0–63	4.59
KLX11A	510.45–510.67	−459	0–63	2.07
KA1596A02	4.32–5.00	−220	63–125	4.36
KLX08	218.54–218.75	−165	63–125	3.77
KLX09	720.15–720.30	−691	63–125	1.06
KLX13A	494.37–494.84	−466	250–500	5.01
KLX13A	578.03–578.56	−550	250–500	5.01
KLX13A	494.37–494.84	−466	500–1000	5.03
KLX13A	531.98–532.66	−503	500–1000	5.10
KLX13A	578.03–578.56	−550	500–1000	5.05

2.2.4 Desorption experiments using standard $Co(NH_3)_6^{3+}$-method

In the standard ISO 23470:2007 one-step method the samples are saturated with a 0.0166 M $Co(NH_3)_6Cl_3$ solution. The $Co(NH_3)^{3+}$ ion is a strongly adsorbing ion, which saturates all exchangeable cation sites on the sample. Thus, the loss of Co can be measured directly from the solution and will represent the CEC. The desorbed cations can be measured from the same solution and should correspond to the loss of Co. Slight modifications to the method have been made due to the small sample sizes.

Sample massess between 1.4–7 g of dried and sieved fracture coating minerals from bore holes KLX08, KLX11A, KLX13A, KLX16A, see Table 2-5, were used for the experiments. The samples were prepared according to the standard method ISO 23470:2007, with minor modifications: the samples were soaked in 0.0166 mol/L $Co(NH_3)_6Cl_3$ solution and shaken for one hour. Thereafter, the samples were centrifuged and the supernatant collected for the determination of exchanged cations with ICP-OES. One blank sample without added sample was prepared and treated in the same way as the samples. No replicate samples could be made due to the small sample sizes.

The standard method requires the use of a minimum sample mass of 10 g for samples low in humus and clays and 1.32 g for samples with high clay contents. Since the collected sample sizes in this study in some cases were below the mass required by the standard. the results obtained here might have larger spreading and uncertainties.

Table 2-5. List of samples, sample drill core depths, grain size fraction and sample mass used in the $Co(NH_3)_6^{3+}$-experiments.

Drill core	Drill core length (m)	Elevation (m.a.s.l.)	Grain size (µm)	Sample mass (g)
KLX16A	33.95–34.20	−11	0–63	4.23
KLX08	218.54–218.75	−165	0–63	4.11
KLX13A	531.98–532.66	−503	0–63	1.67
KLX16A	33.95–34.20	−11	63–125	2.46
KLX11A	510.45–510.67	−459	63–125	1.35
KLX13A	578.03–578.56	−550	63–125	6.99
KLX13A	494.37–494.84	−466	250–500	5.02
KLX13A	578.03–578.56	−550	250–500	5.00
KLX13A	494.37–494.84	−466	500–1000	5.01
KLX13A	578.03–578.56	−550	500–1000	5.02
KLX13A	531.98–532.66	−503	500–1000	5.02

2.3 Analyses

2.3.1 Mineral characterisation

XRD

Identification of major minerals using X-ray diffraction was made on two different fractions of the fracture coating material. Sieved samples were analysed at the Geological Survey of Sweden (SGU), while un-sieved samples, including all grain size fractions, were studied at Stockholm's University (SU). The reason for using the two laboratories was to compare the outcome of the methodologies used in the two laboratories.

The samples analysed at SGU were prepared and analyzed according to the method described by Drever (1973). The samples were grinded with an agate mortar and then mixed with deionized water. Thereafter, sodium hexametaphosphate (65–70 % Sigma-Aldrich) solution was added to the mixture (to avoid flocculation) and the particle aggregates were separated through ultrasound dispersion. The suspension was then allowed to settle and the upper, non-sedimented part was removed and filtered through a Millipore filter (0.2 µm) and the collected solid was smeared onto a glass slide. After drying, the sample was analyzed by XRD and thereafter saturated with ethylene glycol prior to a second measurement. The ethylene glycol saturation step was made for identification of possible (structurally) expanding phases. As a last step and prior to a third measurement, the sample (smeared on a glass slide) was dried in 400 °C for 1.5 h and cooled to room temperature.

The samples analysed at SU were dried and grinded with an agate mortar prior to XRD analysis. In this method, several grams of sample were used for mineral identification and interpretation of the data was carried out using the software X´Pert data Collection and HighScore Plus. The XRD used for the analyses was a Panalytical X´Pert Alpha 1 powder diffractometer set in Theta-2Theta geometry and equipped with a focusing Johansson Ge monochromator producing pure Cu-Kα1 radiation. The tube position is fixed while the PIXCEL detector is moving.

SEM-EDS

For most samples SEM-EDS (Scanning Electron Microscopy – Electron Dispersive Spectrometry) was used to estimate the elemental composition and to investigate the mineralogy of the samples. The analyses were performed on non-pretreated and uncoated grains. All measurements were performed at the Department of Geological Sciences, Stockholm's University on a Fei Quanta 650 FEG equipped with a Backscatter and an Electron Dispersive Spectrometry Detector (EDS Detector) was used for all measurements. Both high and low vacuum were used for the analyses. Data processing software was Oxford AZtec and Oxford Inca using Oxford Tru-Q technology. Detection limit ~0.1 wt% Instrument calibration was made every second hour on a cobolt standard and all measurements were normalized to 100 %. SEM-EDS is a semi-quantitative technique that gives a good approximation and general overview over the sample character but has a relative uncertainty of up to 5 %. Therefore, SEM-EDS may not be used for any exact mineralogical or compositional determinations and should therefore be considered indicative rather than precise especially for samples with uneven morphology, like the samples used.

B.E.T. Surface Area Determinations

Surface area analyses were made on a Micromeritics ASAP using high purity N_2 gas for adsorption. No sample preparation was used prior to the analyses, except degassing at 105 °C overnight to remove adsorbed water and gases (ISO 12570:2000).

2.3.2 Analysis of liquid phases (ICP-OES)

All samples were mixed with 5 µL concentrated HNO_3 (puriss. Sigma Aldrich) to retain all metals in solution and avoid precipitation prior to the ICP-OES analyses. All $Co(NH_3)_6^{3+}$ samples had to be analyzed without the added HNO_3, because of the occasional occurrence of precipitations that disturbed the ICP-system. This was not considered as a major problem since all $Co(NH_3)_6^{3+}$ samples were prepared immediately before analysis, minimizing effects of precipitation. The analyses were performed on a Varian Vista AX from Agilent Technologies with the analytical uncertainty 5 % and detection limit according to Table 2-6. Standards used for instrument calibration are LGC-Promochem Multi element standards for major and minor cations.

Table 2-6. Detection limits for selected elements for ICP-OES analyses.

Element	Detection limit (ppb)
Al	3.96
Ca	0.06
Co	3.61
Fe	2.96
K	2.31
Mg	0.08
Mn	0.53
Mo	5.21
Na	0.90
Ni	10.3
Si	3.89
Sr	0.05
Ti	0.84
Zn	1.81

3 Results and discussion

3.1 Solid characterization

Similar results were obtained from the XRD and SEM-EDS methods used for mineral identification but quantification is not possible with these techniques. Most samples consisted of mainly chlorite (dominantly clinochlore, but sometimes with high Fe concentrations = chamosite) and some also contained various amounts of calcite, hematite, quartz and clay minerals such as smectite, see Table 3-1 and Section 3.1.1.

Table 3-1. List of sieved samples and their mineralogy measured with SEM-EDS and XRD. Wall rocks are described in Wahlgren et al. (2008), Carlsten et al. (2007) and Winberg (2010).

Drill core	Elevation (m.a.s.l.)	Drill core length (m)	Sieved grain size (µm)	Mineralogy (SEM-EDS. XRD)	Clays	Wall rock
KLX08	−165	218.54–218.75	0–125	Chlorite (clinochlore, dominating), quartz, calcite, K-feldspar, plagioclase.	Dominating: chlorite (clinochlore). Minor amounts of Illite, biotite.	Ävrö granite
KLX09	−691	720.15–720.30	63–125	Chlorite (dominating), K-feldspar, calcite, quartz, goethite.	Dominating: chlorite. Minor amounts of chlorite-smectite (resembling corrensite).	Ävrö granite
KLX11A	−459	510.45–510.67	0–125	Chlorite (clinochlore, dominating), epidote, quartz, kaolinite, K-feldspar (adularia).	Dominating: chlorite (clinochlore). Minor amounts of chlorite-smectite (resembling corrensite).	Ävrö granite
KLX13A	−466	494.37–494.84	0–125	Chlorite (clonochlore, dominating) quartz, calcite, hematite, illite.	Chlorite (clinochlore) totally dominating.	Ävrö granite
	−503	531.98–532.66	0–125	Chlorite (clinochlore, dominating), calcite, quartz, hematite, apatite.	Dominating: smectite-chlorite type with large amounts of corrensite and minor amounts of chlorite.	
	−550	578.03–578.56	0–63	Chlorite, corrensite, quartz, calcite, hematite, albite.	Chlorite (dominating), minor amounts of smectite-chlorite.	
KLX16A	−11	33.95–34.20	250–500	Chlorite (clinochlore, dominating), calcite, K-feldspar (adularia), hematite.	Chlorite (clinochlore) dominating, minor amounts of smectite-chlorite.	Ävrö granite
KA1596A02	−220	4.32–5.00	0–63	Chlorite (dominating), zeolite/quartz, calcite.	Chlorite dominating, minor amounts of smectite-chlorite.	Äspö Diorite

3.1.1 SEM-EDS

KLX09

The dominant mineralogy of the sample from KLX09 is presented in Table 3-1, Figure 3-1 and Figure 3-2 and Table A-1 (Appendix). Spot analysis spectra 1, 6, 7 and 9 representing the brighter areas in Figure 3-1 have a calculated molecular formula close to Fe-oxide or Fe-oxyhydroxide but with some components of C and Si as well. The gray areas (spectrum number 3, 4, 5 and 8) have a calculated molecular formula close to clinochlore ($(Mg_5Al)(AlSi_3)O_{10}(OH)_8$) and calcium carbonate ($CaCO_3$). A close connection to carbonates is found in all analyses (spot analyses and mapping).

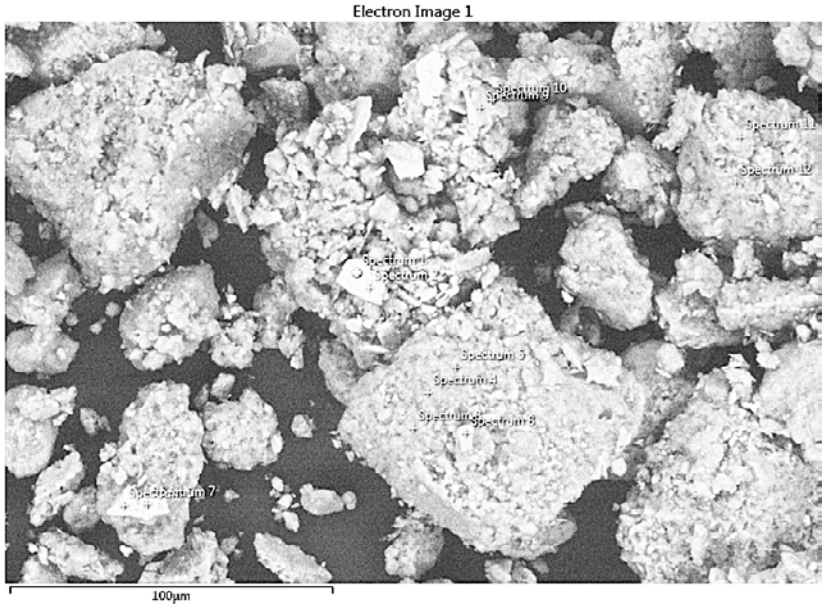

Figure 3-1. *SEM-EDS picture of a KLX09 sample.*

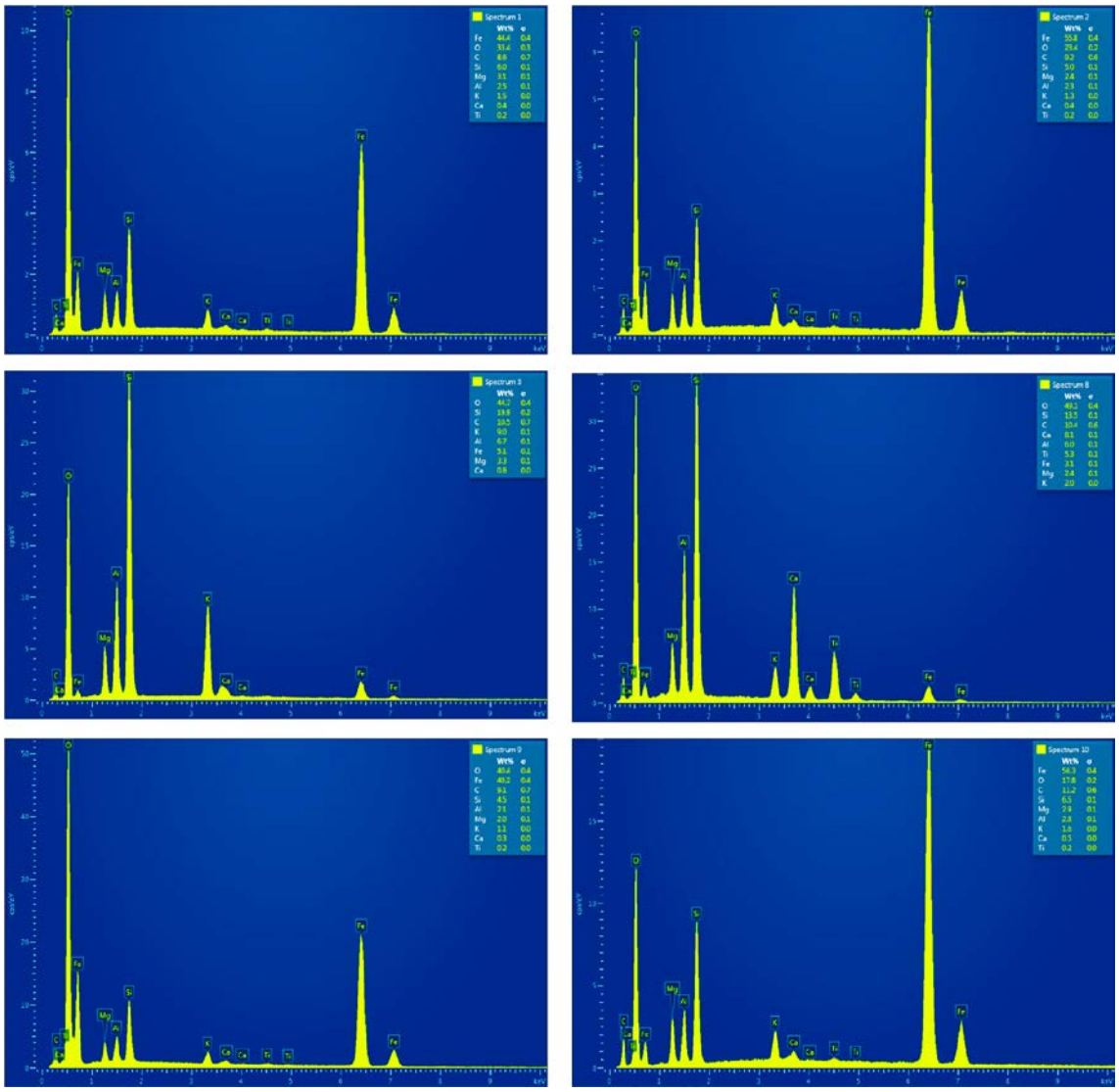

Figure 3-2. *SEM-EDS-spectra showing the elemental distribution in the major mineral phases in the KLX09 sample. Data listed in Table A-1 (Appendix).*

KLX11A

The dominant clay mineralogy when analyzed as a dry sample is a Fe-rich chlorite phase ($(Mg,Fe^{2+})_5Al(AlSi_3O_{10})(OH)_8$).

The SEM-EDS analyses showed that spot analyses and showed that the clay minerals were covering the whole surfaces of the larger grains and sometimes even form larger clusters of clays, see Figure 3-3a and Figure 3-4 (in which the average of at least three spot analyses are presented) and Table A-2 (Appendix). Analyses at higher magnification indicated the presence of chlorite, calcite, clay minerals and apatite, Figure 3-3.

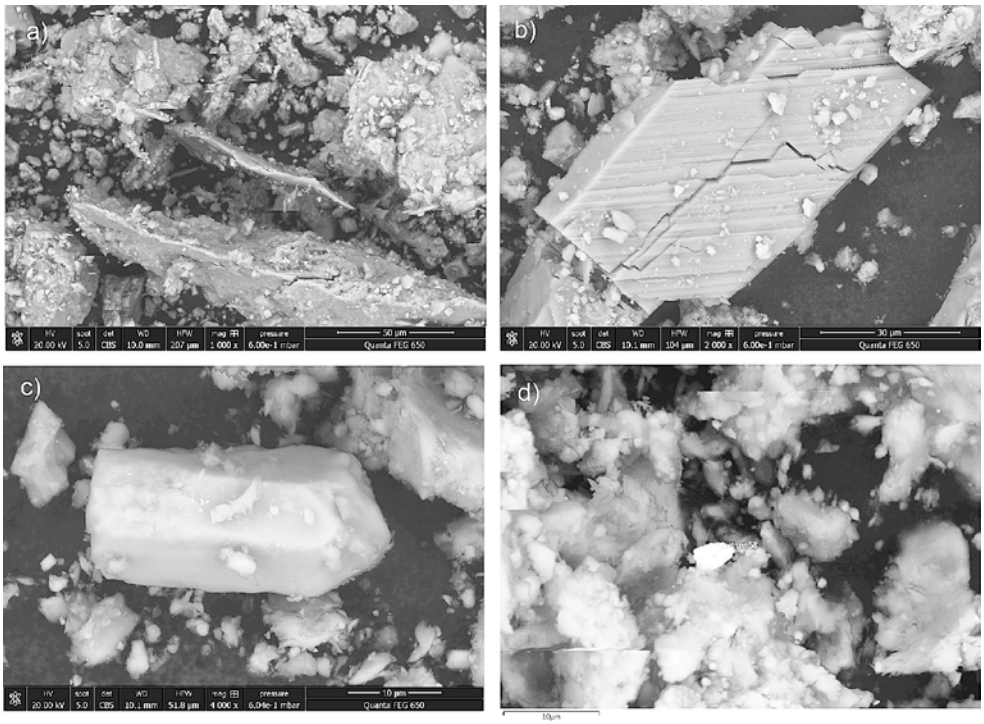

Figure 3-3. *SEM-EDS overview picture of mineral grains with sizes less than 400 µm in the KLX11A sample. There are different types of grains a) clinochlore (dominant species) b) calcite c) apatite and d) occasionally occurring metal-rich grains.*

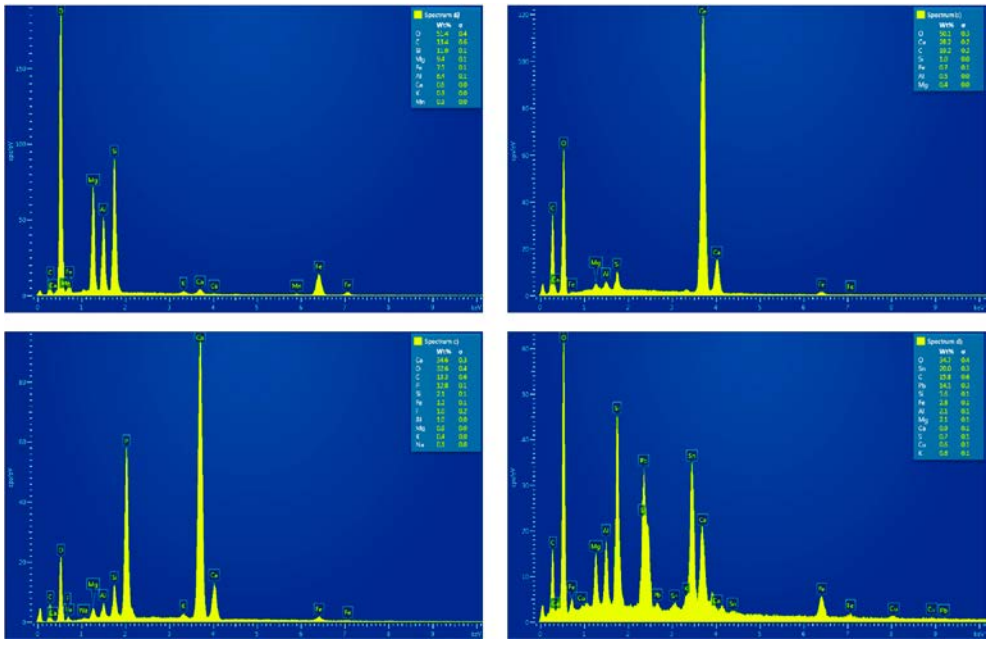

Figure 3-4. *SEM-EDS-spectra showing the elemental distribution in the major mineral phases in the KLX11A sample shown in Figure 3-3. Data listed in Table A-2 (Appendix).*

KLX13A (494)

The dominant clay mineralogy of KLX13A (494) when analyzed as a dry sample is a Mg-rich chlorite phase ($(Mg,Fe^{2+})_5Al(AlSi_3O_{10})(OH)_8$) but with hematite and corrensite as well Figure 3-5, Figure 3-6 and Table A-3 (Appendix).

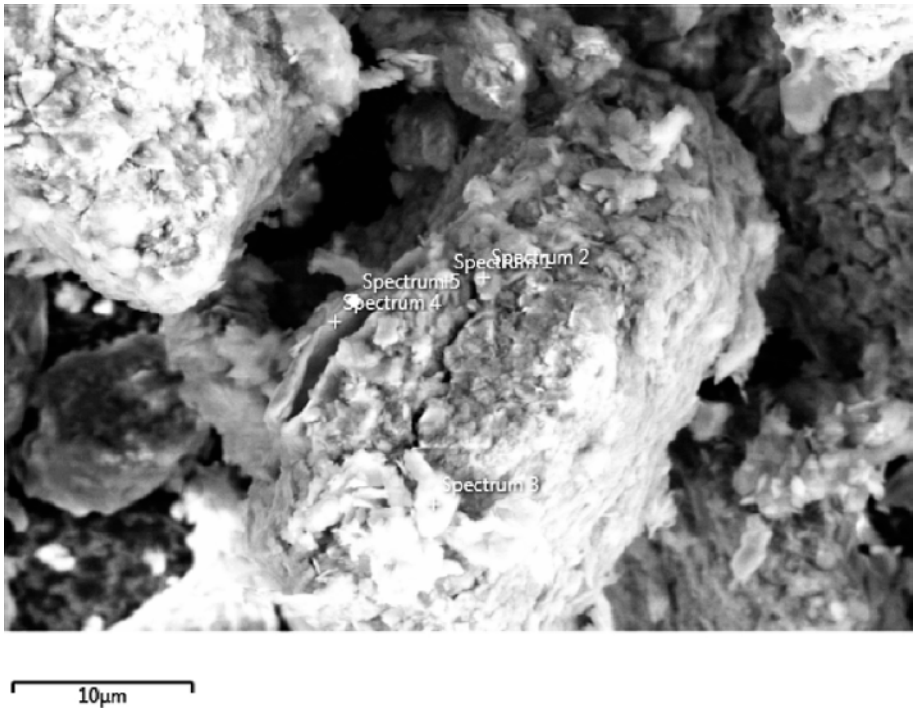

Figure 3-5. *SEM-EDS overview picture of grains in KLX13A (494). The different types of grains are clinochlore (dominant species), hematite (spectrum 3), corrensite (spectra 1–2, 4–5).*

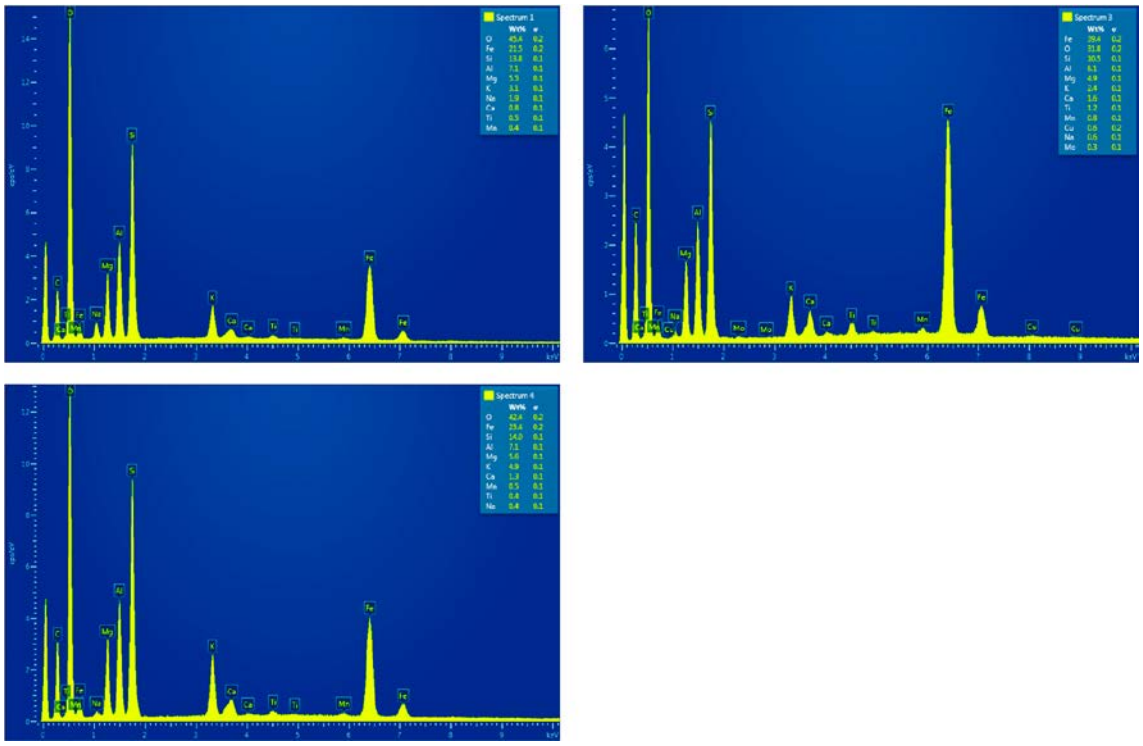

Figure 3-6. *SEM-EDS-spectra showing the elemental distribution in the major mineral phases in the KLX13A (494) sample shown in Figure 3-5. Data listed in Table A-3 (Appendix).*

KLX13A (531)

The dominant clay mineralogy of KLX13A (531) when analyzed as a dry sample is a Mg-rich chlorite phase ($(Mg,Fe^{2+})_5Al(AlSi_3O_{10})(OH)_8$).

The samples were analyzed with SEM-EDS and showed that the clay minerals were covering the whole surfaces of the larger grains but both calcite and pyrite crystals could be distinguished, see Figure 3-7 and Figure 3-8 and Table A-4 (Appendix).

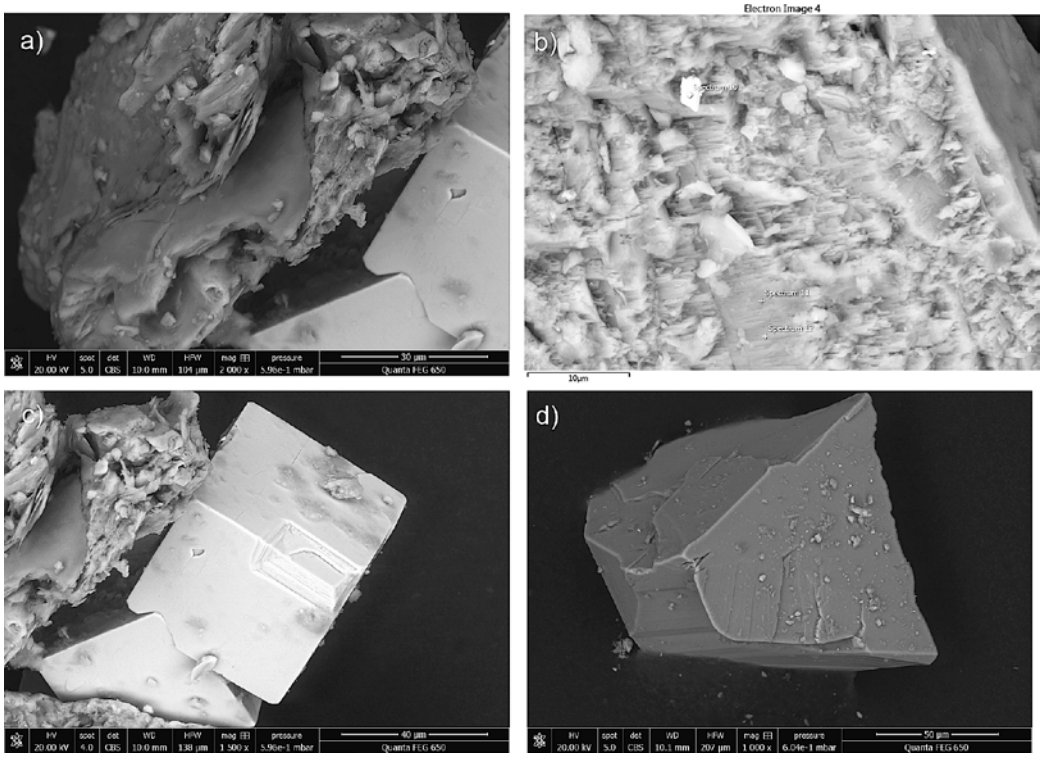

Figure 3-7. *SEM-EDS overview picture of grains in KLX13A (531). The different types of grains are a) clinochlore (dominant species) b) zircon (the bright mineral) c) pyrite and d) calcite.*

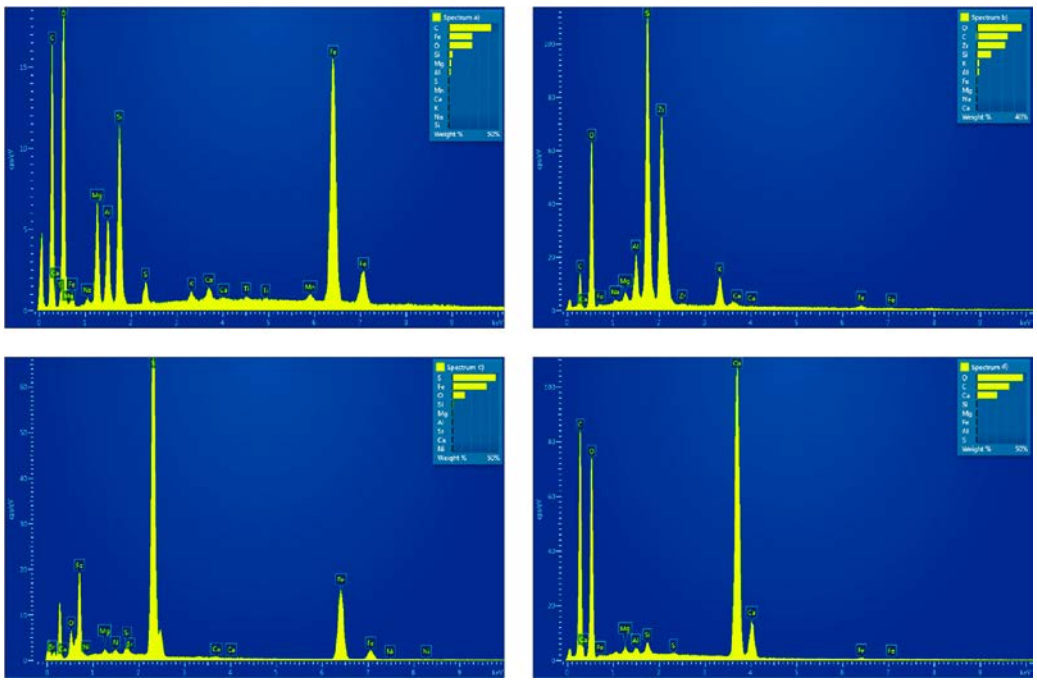

Figure 3-8. *SEM-EDS-spectra showing the elemental distribution in the mineral phases in the in KLX13A (531) sample shown in Figure 3-7. Data listed in Table A-4 (Appendix).*

KLX13A (578)

The dominant clay mineralogy of KLX13A (578) when analyzed as a dry sample is a Mg-rich clinochlore phase ($(Mg,Fe^{2+})_5Al(AlSi_3O_{10})(OH)_8$).

ESEM showed that most crystals within the sample are subhedral with minor amounts of euhedral crystals such as pyrites or calcites, see Figure 3-9, Figure 3-10 and Table A-5 (Appendix). Instead, small, irregular crystals are widespread and the elemental composition is the only way to identify the mineralogy, with ESEM. Some grains contain high Ni, Fe and Cr and could possibly be fractions from the core drilling equipment.

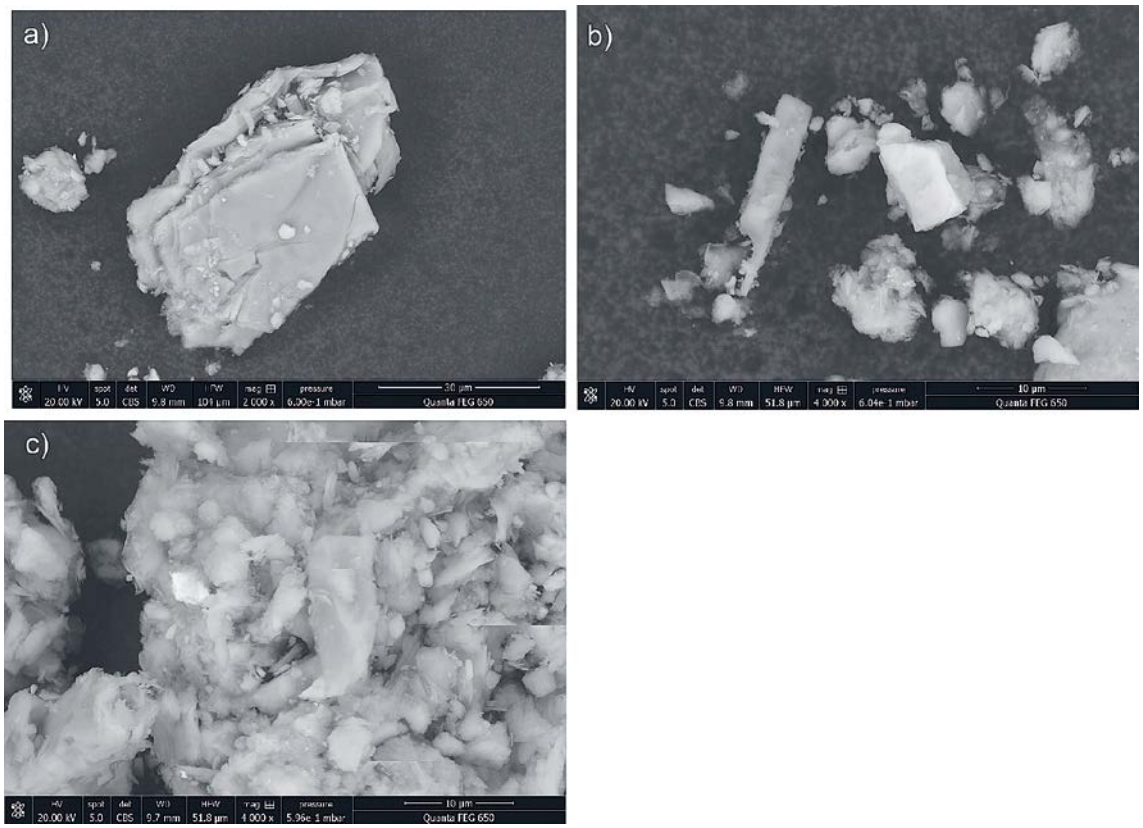

Figure 3-9. *SEM-EDS overview picture of grains in KLX13A (578). The different types of grains are a) clinochlore (dominant species) b) plagioclase and c) clay minerals.*

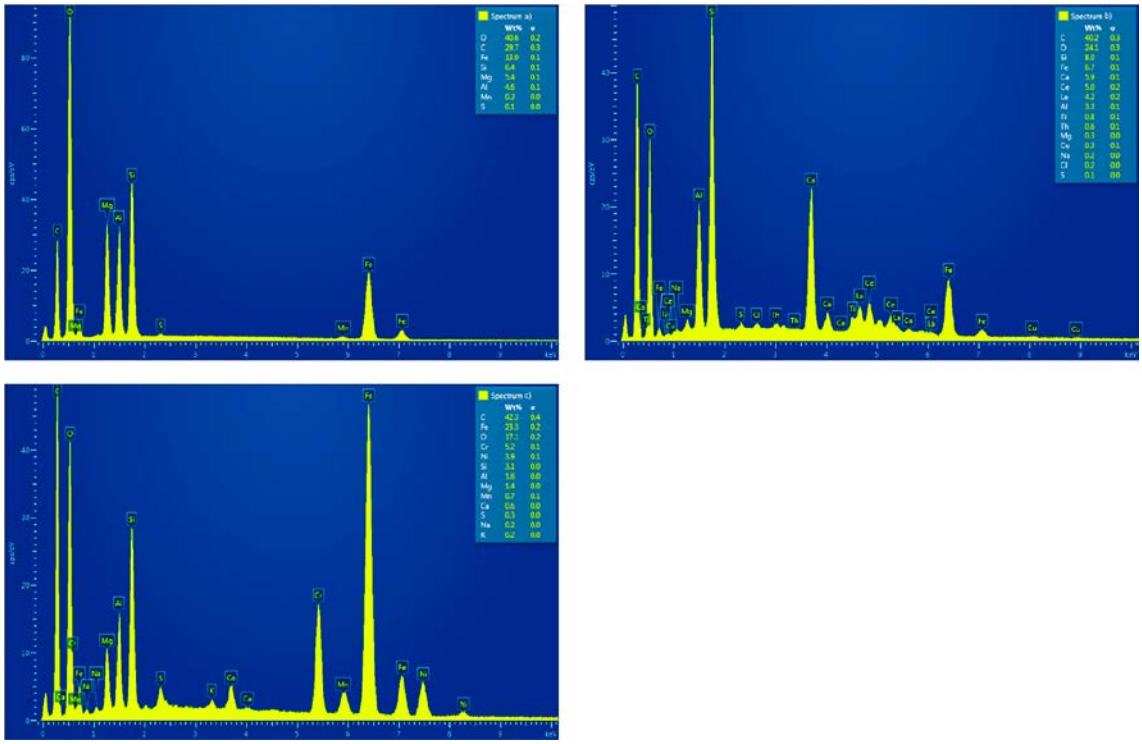

Figure 3-10. *SEM-EDS-spectra showing the elemental distribution in the major mineral phases in the KLX13A (578) sample shown in Figure 3-9. Data listed in Table A-5 (Appendix).*

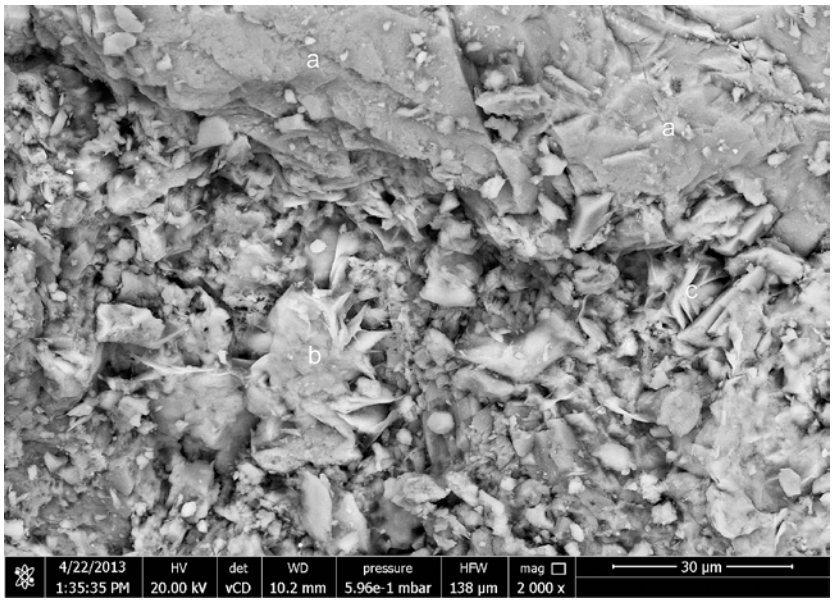

Figure 3-11. *SEM-EDS picture of the sample KLX13A (578) grain surface. Minerals indicated are a) calcite b) iron oxide and c) clays.*

3.1.2 B.E.T.

KLX13A samples were taken from three depths, see Table 3-1; two of these samples showed a surface area of around 8 m^2/g while the sample from 531.98–532.66 m had almost a doubled surface area of ~14 m^2/g (Table 3-2). The material from both KLX11A and KA1596A02 had similar surface areas of ~10–11 m^2/g (Table 3-2).

Table 3-2. B.E.T. surface area measurements at different depths (m).

Drill core	Drill core length (m)	Elevation (m.a.s.l.)	B.E.T. surface area (m^2/g)
KA1596A02	4.32–5.00	−220	10.10 ± 0.01
KLX11A	510.45–510.67	−459	11.10 ± 0.02
KLX13A	494.37–494.84	−466	8.42 ± 0.01
KLX13A	531.98–532.66	−503	14.3 ± 0.02
KLX13A	578.03–578.56	−550	8.57 ± 0.01

3.2 Cation-Exchange measurements

3.2.1 Flow-through experiments

The use of pure water for the leaching of fracture coating material with the grain size fraction 125–250 µm resulted in extremely high cation concentrations in the effluent (Table 3-3), most likely due to dissolution of the material, both calcite and the other minerals in the samples. Because of the high dissolution, the numbers do not represent CEC and will be denoted here as CEC_{dis}. Especially Al, Fe, Mg and Na are exceptionally high compared with any other technique indicating that the dissolution of the material is profound. All the experiments on fracture coating material with the grain size fraction 0–125 µm resulted in such high CEC_{dis} that they are not further discussed. Interestingly, there is a decrease in CEC_{dis} with ionic strength in sample KLX09, which is not seen in the other samples. Usually, the dissolution of calcite increases with increasing ionic strength or remains unchanged (Krauskopf 1979). However, in the study of Ruiz-Agudo et al. (2010), which reports the dissolution rate of calcites at different ionic strengths, there is a clear decrease in the etch pit spreading rate on calcite when comparing KCl solutions of 0.001 M and 0.01 M. At KCl concentrations from 10 mM to 100 mM, the dissolution rate increases again. Our study appears to confirm the decrease in dissolution rate when going from a KCl concentration of 1 mM to 10 mM, see Table 3-3.

Table 3-3. CEC_{dis} of samples subjected to flow-through. Milli-Q leaching experiments. CEC_{dis} is presented both with and without Ca, and (Ca+K) to illustrate the effect of these elements on the total CEC_{dis}.

Drill cores	Drill core length (m)	Grain size (µm)	KCl (M)	CEC_{dis} (meq/100 g)	CEC_{dis}−Ca (meq/100 g)	CEC_{dis}−(Ca-K) (meq/100 g)	Ca (mmol/g)
KLX09	720.15–720.30	0–125	0.001	1460 ± 73	1107 ± 55	773 ± 39	1.76
KLX09	720.15–720.30	0–125	0.010	1417 ± 71	826 ± 41	206 ± 10	2.96
KLX09	720.15–720.30	0–125	0.020	683 ± 34	353 ± 18	58.3 ± 3	1.67
KLX13A	494.37–494.84	0–125	0	1377 ± 69	574 ± 29	531 ± 27	8.04
KLX13A	578.03–578.56	0–125	0	2019 ± 101	1166 ± 58	1105 ± 55	8.54
KLX13A	494.37–494.84	125–250	0	360 ± 18	208 ± 10	–	0.76
KLX13A	578.03–578.56	125–250	0	370 ± 19	297 ± 15	–	0.36
KLX16A	33.95–34.20	0–125	0.001	726 ± 36	334 ± 17	161 ± 8	1.97
KLX16A	33.95–34.20	0–125	0.010	779 ± 39	195 ± 10	62.7 ± 3	2.92
KLX16A	33.95–34.20	0–125	0.020	638 ± 32	288 ± 14	20.5 ± 1	1.47

The time-dependent elemental leaching of the elements from the samples into the water is shown in Figure 3-13 to Figure 3-14. Already after 50–80 minutes, the leaching of elements into the water has reached a steady state. All analyzed elements behave similarly with a high element release during the first 1–5 minutes. The Fe, Mg, Al, K and Ca concentrations are exceptionally high, which indicates dissolution of calcite, chlorite, clays and/or iron oxides. A flow-through system is an illustrative way to follow the elemental release as a function of time and could hold a great potential for future studies of CEC, using standard CEC chemicals (Ross and Ketterings 2011, ISO 13536:1995, ISO 23470:2007) instead of water.

Data on the leaching of cations with time are presented in the Appendix.

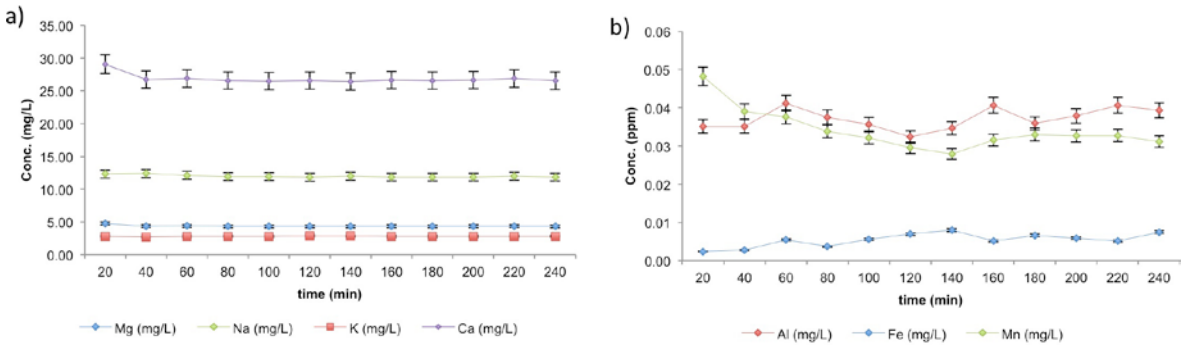

Figure 3-12. *Desorbed exchangeable cations as a function of time for sample KLX13A 494.37–494.84 m, grain size fraction 0–125 µm, using water as a leaching medium: a) leaching of Mg, Na, K and Ca; b) leaching of Al, Fe, and Mn.*

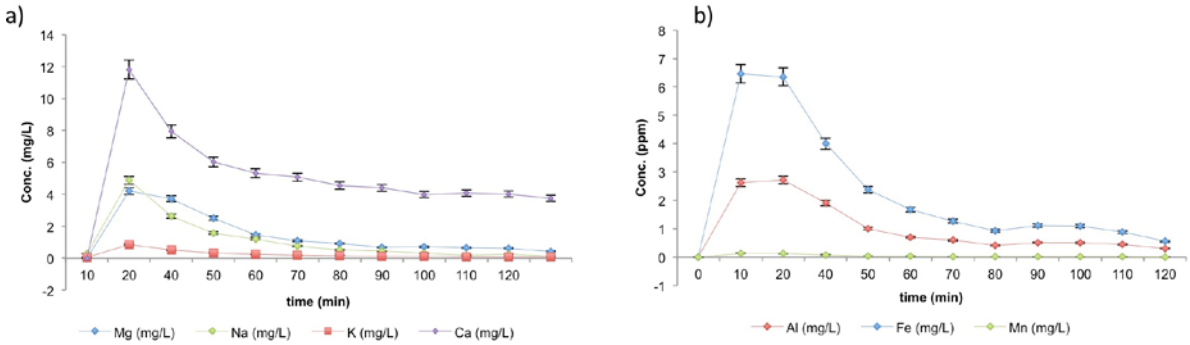

Figure 3-13. *Desorbed exchangeable cations as a function of time for sample KLX13A 494.37–494.84 m, grain size fraction 125–250 µm using water as a leaching medium: a) leaching of Mg, Na, K and Ca; b) leaching of Al, Fe, and Mn.*

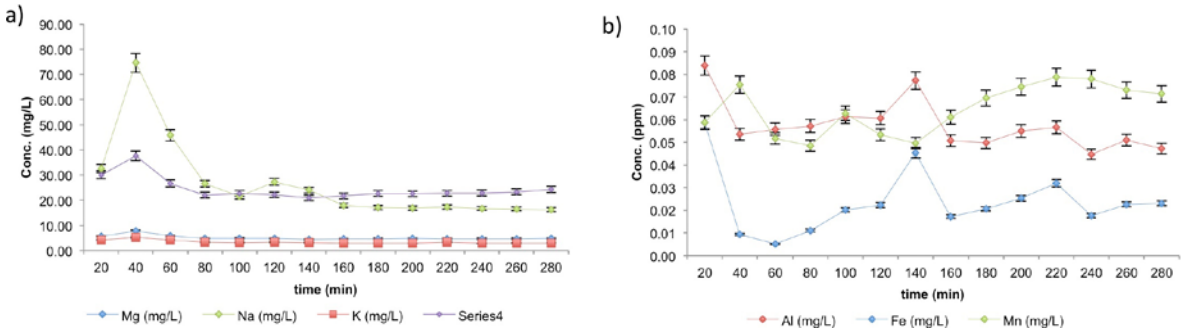

Figure 3-14. *Desorbed exchangeable cations as a function of time for sample KLX13A 578.03–578.56 m, grain size fraction 0–125 µm, using water as a leaching medium: a) leaching of Mg, Na, K and Ca; b) leaching of Al, Fe, and Mn.*

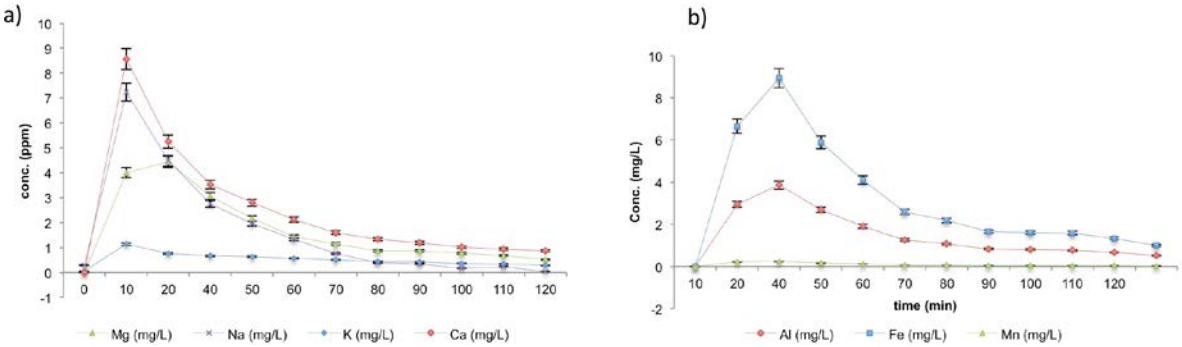

Figure 3-15. *Desorbed exchangeable cations as a function of time for sample KLX13A 578.03–578.56 m, grain size fraction 125–250 µm, using water as a leaching medium: a) leaching of Mg, Na, K and Ca; b) leaching of Al, Fe, and Mn.*

3.2.2 $BaCl_2$ exchange

The standard method for CEC measurement with $BaCl_2$ was used for samples KLX09, KLX13A and KA1596A02 listed in Table 2-3. The expected CEC values were around 20–130 meq/100 g sample (Stumm and Morgan 1981, Faure 1998), however, the obtained values from these experiments were in the range 13.1–53.0 meq/100 g.

This method involves a second step in which the adsorbed Ba^{2+} ions are exchanged with Mg^{2+} ions and in which the decreased concentration of Mg^{2+} correspond to the amount of Ba that is desorbed. However, all results from the ICP-OES measurements showed that the decrease in Mg^{2+} concentration could not be observed, which, similar to Byegård and Tullborg (2012) means that the replacement with Mg^{2+} is not fulfilled on these kinds of samples. The uncertainty of the ICP-OES measurements is approx. 5 %.

Therefore, only the leaching of exchangeable cations through the first step of the ISO 13536:1995 method is represented in Table 3-4. No clear change in CEC with grain size could be observed, see Figure 3-16. A comparison of these data with those obtained from the flow-through experiments (Table 3-3) shows that calcite dissolution and mineral weathering reactions are much less prominent in 1 M $BaCl_2$ as compared with the flow through solutions (deionized water and KCl < 0.02 M).

Table 3-4. CEC from the release of cations in the presence of 1 M $BaCl_2$ for samples of different depths and grain size fractions. The CEC is also presented without Ca to illustrate the effect of these elements on the total CEC.

Drill cores	Drill core length (m)	Grain size (µm)	CEC (meq/100 g)	CEC-Ca (meq/100 g)
Blank			2.42 ± 0.12	1.43 ± 0.07
KLX09	720.15–720.30	0–63	53.0 ± 2.65	8.93 ± 0.45
KLX13A	578.03–578.56	0–63	27.1 ± 1.36	6.28 ± 0.31
KA1596A02	4.32–5.00	0–63	45.4 ± 2.27	4.09 ± 0.20
KLX13A	494.37–494.84	63–125	13.1 ± 0.65	2.79 ± 0.14
KLX13A	531.98–532.66	63–125	49.3 ± 2.47	7.75 ± 0.39
KLX13A	494.37–494.84	250–500	29.0 ± 1.45	4.10 ± 0.21
KLX13A	578.03–578.56	250–500	19.9 ± 0.99	7.32 ± 0.37
KLX13A	494.37–494.84	500–1000	23.8 ± 1.19	3.17 ± 0.16
KLX13A	531.98–532.66	500–1000	47.9 ± 2.39	16.2 ± 0.81
KLX13A	578.03–578.56	500–1000	16.1 ± 0.80	6.52 ± 0.33

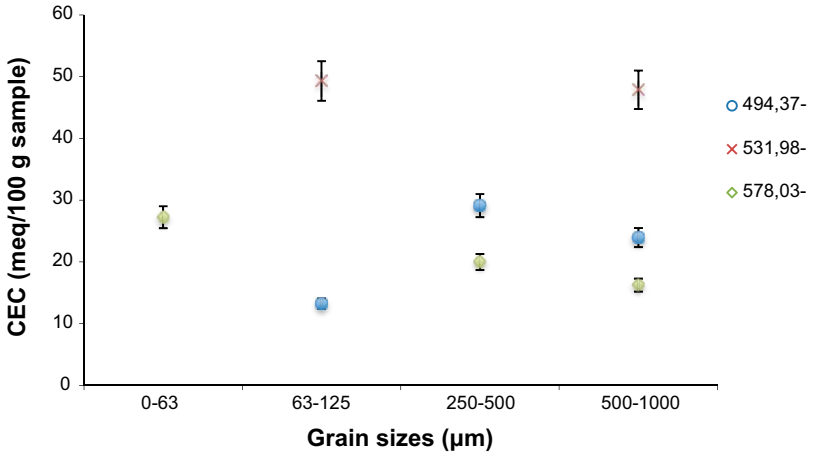

Figure 3-16. *CEC measured (as released cations in the presence of 1 M $BaCl_2$) as a function of grain size from KLX13A from different drill core lengths.*

3.2.3 $Co(NH_3)_6Cl_3$ exchange

All samples had a CEC value between −5.11 and +52.1 meq/100 g, see Table 3-5 and Figure 3-17. Sample KLX13A (531.98–532.66 m) shows a higher CEC than the other samples, which is likely due to the large amount of corrensite and clays in the samples and the concomitant higher B.E.T. (Table 3-2). The high CEC of KLX11A can be explained by the presence of kaolinite. It may be concluded that the dissolution of calcite was either non-existing or very low. The concentration of Ca in the solution was an order of magnitude lower in all analyzed solutions than in all the other methods.

There is a slight trend of a larger CEC (except KLX13A 578.03–578.56 m) with larger grain size fractions, see Figure 3-18. This is likely due to the smaller sample sizes for the smaller grain size fractions, leading to a larger uncertainty and a smaller CEC.

The yellow precipitates forming through the addition of HNO_3 that disturbed the ICP analyses is perhaps $[Co(NH_3)_6](NO_3)_3$ which is reported to precipitate when nitric acid is added to solutions of hexaamminecobalt(III) chloride, see for example (Sutherland 1928, pp 135–136, Farhadi and Pourzare 2012).

Table 3-5. CEC (meq/100 g sample) from the $Co(NH_3)_6Cl_3$ method for samples of different depths and grain size fractions. The uncertainty of the measurements is a combination of the detection limit of the ICP-OES analyses presented in Table 2-6 and an analytical uncertainty of 4 %.The detection limit for CEC is calculated to be 0.92 meq/100 g.

Sample number	Sample mass (g)	Sample name	Drill core length (m)	Sample grain size (µm)	CEC (meq/100 g)
Blank	0.00	Blank			14.6 ± 12.5
1	4.11	KLX08	218.54–218.75	0–63	6.09 ± 5.75
2	4.23	KLX16A,GE003	33.95–34.20	0–63	2.87 ± 5.74
3	1.67	KLX13A	531.98–532.66	0–63	30.9 ± 13.3
4	2.46	KLX16A,GE003	33.95–34.20	63–125	1.62 ± 10.0
5	1.35	KLX11A	510.45–510.67	63–125	11.3 ± 17.9
6	6.99	KLX13A	578.03–578.56	63–125	8.90 ± 3.12
Blank	0.00	Blank			−47.0 ± 27.3
7	5.02	KLX13A	494.37–494.84	250–500	−5.11 ± 5.22
8	5.00	KLX13A	578.03–578.56	250–500	12.7 ± 4.34
9	5.01	KLX13A	494.37–494.84	500–1000	9.74 ± 4.48
10	5.02	KLX13A	531.98–532.66	500–1000	52.1 ± 2.36
11	5.02	KLX13A	578.03–578.56	500–1000	−1.25 ± 5.02

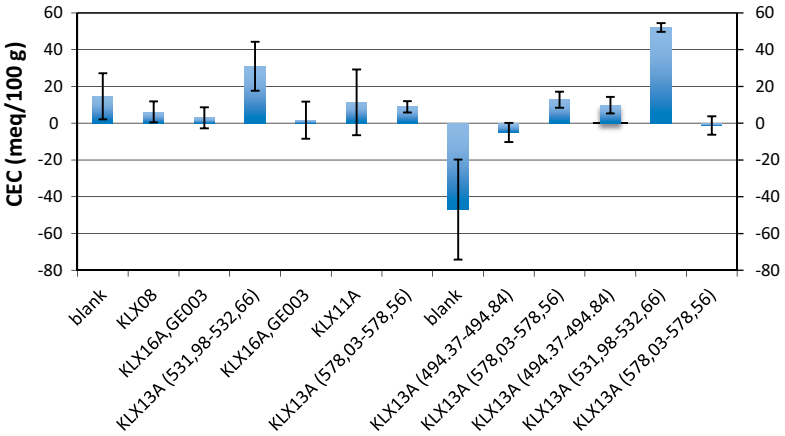

Figure 3-17. *CEC (meq/100 g sample) from the $Co(NH_3)_6Cl_3$ method for samples of different drill core lengths and grain sizes. Two of the samples (both from KLX16A) showed dissolution of Co into solution. The uncertainty of the measurements is a combination of the detection limit of the ICP-OES analyses presented in Table 2-6 and an analytical uncertainty of 4 %.*

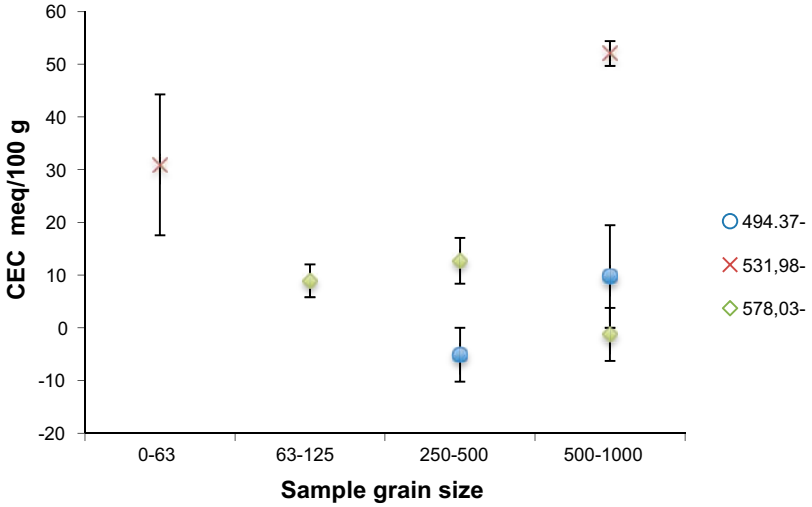

Figure 3-18. *CEC (meq/100 g sample) measured with the batch $Co(NH_3)_6Cl_3$ method as a function of grain size for samples KLX13A at different drill core lengths.*

3.2.4 NH_4Ac

All analyzed samples gave a higher CEC than with the other methods, see Table 3-6, most likely due to the dissolution of calcite (Eq. 3-1), causing a high and overestimated CEC.

$$CaCO_{3(s)} + NH_4^+ = Ca^{2+} + HCO_3^- + NH_3 \qquad \text{(Eq. 3-1)}$$

This method results in 53 % higher CEC than the $BaCl_2$-method and 79 % higher CEC than the Co-hexaammine method. However, if the Ca^{2+} ions are not included in the CEC calculations, the values decrease considerably. When Ca is excluded from the total CEC, the values are comparable with the $Co(NH_3)_6^{3+}$-method. It is however important to point out that a CEC of a sample without the Ca^{2+} ion will most likely give an underestimation of the CEC.

Figure 3-19 shows the CEC obtained with this method plotted against grain size indicating that there is a general trend of decreasing CEC with grain size.

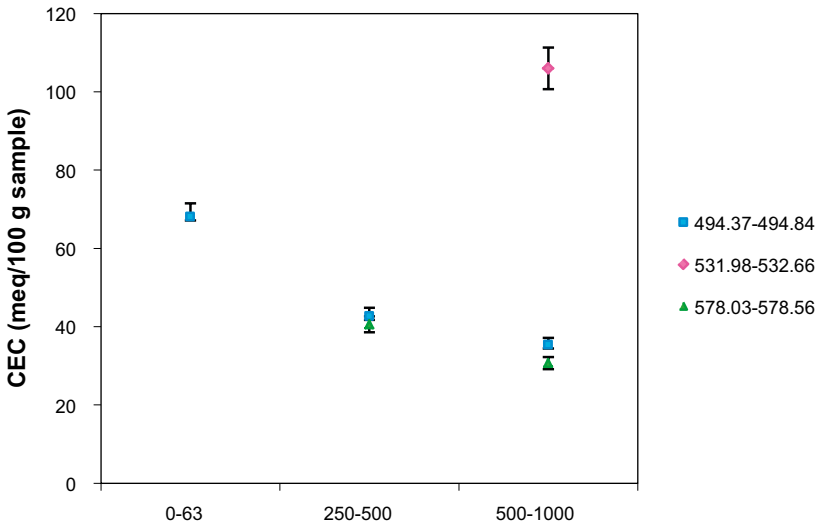

Figure 3-19. *CEC (meq/100 g sample) measured with the batch NH_4Ac method) as a function of grain size for samples KLX13A at different drill core lengths.*

Table 3-6. CEC (meq/100 g sample) obtained with the NH4Ac method for samples of different depths and grain size fractions. The CEC is also presented without Ca and Na to illustrate the effect of these elements on the total CEC.

Drill core	Drill core length (m)	Grain size (µm)	CEC (meq/100 g sample)	CEC-Ca (meq/100 g sample)	CEC-Ca-Na (meq/100 g sample)
Blank			3.13 ± 0.16	2.34 ± 0.12	1.78 ± 0.09
KLX13A	494.37–494.84	0–63	68.1 ± 3.40	8.36 ± 0.42	4.50 ± 0.23
KLX11A	510.45–510.67	0–63	170 ± 8.49	20.2 ± 1.01	9.26 ± 0.46
KA1596A02	4.32–5.00	63–125	89.4 ± 4.47	12.4 ± 0.62	3.37 ± 0.17
KLX04	218.54–218.75	63–125	44.0 ± 2.20	7.98 ± 0.40	5.44 ± 0.27
KLX09	720.15–720.30	63–125	155 ± 7.77	42.0 ± 2.10	18.3 ± 0.92
Blank			0.14 ± 0.01	0.02 ± 0.00	0.02 ± 0.00
KLX13A	494.37–494.84	250–500	42.7 ± 2.13	12.5 ± 0.63	2.60 ± 0.13
KLX13A	578.03–578.56	250–500	40.6 ± 2.03	24.5 ± 1.23	3.29 ± 0.16
KLX13A	494.37–494.84	500–1000	35.4 ± 1.77	9.63 ± 0.48	2.11 ± 0.11
KLX13A	531.98–532.66	500–1000	106 ± 5.30	65.7 ± 3.29	3.94 ± 0.20
KLX13A	578.03–578.56	500–1000	30.7 ± 1.54	18.8 ± 0.94	3.49 ± 0.17

4 Discussion

There are large deviations in the obtained CEC values between the different methods tested and between the grain size fractions, see Table 4-1. The flow-through values are not included in the comparisons because dissolution reactions resulted in high cation concentrations (CEC_{dis}), from which the cation exchange properties of the minerals could not be derived. The best agreement between the methods is among the larger grain sizes (250–1000 µm), in which the CEC of all samples is less or equal 106 meq/100 g whereas the CEC among the smaller grain sizes is up to 170 meq/100 g. The NH_4Ac method shows much higher CEC values than the other two methods and it can be concluded that this method is not suitable for the type of samples used in this study because of the extensive dissolution of calcite. The $BaCl_2$ method also shows high CEC values but does not dissolve calcite as effectively as the NH_4Ac method.

When comparing CEC in only KLX13A from different depths (Table 4-2) the CEC still has a large spreading among the different methods. It can be seen that the NH_4Ac method gives the highest estimation of the CEC and the $Co(NH_3)_6^{3+}$ method the lowest CEC values. The reason for the observed differences among the samples is likely due to the mineralogy of the samples, especially the calcite content. The highest CEC is measured on KLX13A (531.98–532.66 m) and the main mineralogy in this sample is chlorite, corrensite, calcite, quartz, hematite and apatite. The high amount of clays and the concomitant high B.E.T. value (Table 3-2) is likely the reason why the CEC values are highest in this sample. The high measured CEC in the other methods is likely due to the high content of calcite (obtained by an apparently high CEC caused by the fact that Ca^{2+} originating from dissolved calcite is erroneously interpreted as leached by cation exchange in the method).

It can be concluded that the large differences among the methods used in this study are most likely due to the dissolution of calcite, which results in an overestimation of the CEC. The large variation in the sample masses may also have influenced the outcome. Some sample masses were as small as 1.5 g whereas others were over 10 g. Even though the CEC calculation takes the amount of sample in consideration this is still a factor of uncertainty.

The $Co(NH_3)_6^{3+}$-method gives lowest CEC values and the method is likely most reliable, due to its aversion to dissolve calcite. Previous studies have analyzed the Co-hexaammine method on calcareous clays with good and reliable results (Dohrmann and Kaufhold 2009, Byegård and Tullborg 2012). The method is also quick and only involves a single step. If considering the $Co(NH_3)_6^{3+}$-method to be most reliable, the CEC of all samples are between −5.11 and +52.1 meq/100 g sample. Since all samples contain clay minerals, calcite and chlorites (see Table 3-1) these CEC values are fully reasonable. This is consistent with the CEC for pure chlorites that are reported to vary between 20 and 40 meq/100 g (Allred et al. 2007) and for pure clays with CEC around 90–130 meq/100 g sample. In Byegård and Tullborg (2012), the $Co(NH_3)_6^{3+}$-method resulted in values similar to this study (approx. 14.8 meq/100 g) for similar material.

Higher CEC values are obtained with the $BaCl_2$-method, which is expected due to its susceptibility to dissolve calcite and thus it gives overestimated CEC values. However, the CEC values from the $BaCl_2$-method are within the range of expected CEC values for these kinds of samples. Also, the deviation from the $Co(NH_3)_6^{3+}$-method is 38 % higher for the KLX13A-samples, which is large but not unreasonable since the samples measured are from different depths and/or drill cores.

When plotting the CEC versus depth in the KLX13A samples one can see that there is a general trend of increased CEC with depth down to 531 m and then a small decrease again, see Figure 4-1. All methods show the same trend. The samples analyzed from KLX13A 531.98–532.66 m have all much higher CEC than samples from the other depths (Figure 4-1). A major reason for this deviation is likely due to the higher B.E.T. of these samples (Table 3-2), which is expected due to the higher amount of clay minerals from this drill core sample (Table 3-1).

Table 4-1. Comparison of measured CEC with different methods on all samples at different drill core lengths. In the "INTERVALS" column the blue background color represent the $Co(NH_3)_6^{3+}$-method, green the NH_4Ac method and pink the $BaCl_2$ method.

Drill core	Drill core length (m)	Grain size (µm)	$BaCl_2$ (meq/100 g)	NH_4Ac (meq/100 g)	$Co(NH_3)_6^{3+}$ (meq/100 g)	INTERVALS (meq/100 g)
KLX08	218.54–218.75	0–63			6.09	
KLX13A	531.98–532.66	0–63			30.9	
KLX16A	33.95–34.20	0–63			2.87	2.87–30.9
KLX13A	494.37–494.84	0–63		68.1		
KLX11A	510.45–510.67	0–63		170		68.1–170
KLX09	720.15–720.30	0–63	53			
KLX13A	578.03–578.56	0–63	27.1			
KA1596A02	4.32–5.00	0–63	45.4			27.1–53
KLX11A	510.45–510.67	63–125			11.3	
KLX13A	578.03–578.56	63–125			8.90	
KLX16A	33.95–34.20	63–125			1.62	1.62–11.3
KA1596A02	4.32–5.00	63–125		89.4		
KLX04	218.54–218.75	63–125		44		44.0–89.4
KLX09	720.15–720.30	63–125		–		
KLX13A	494.37–494.84	63–125	13.1			
KLX13A	531.98–532.66	63–125	49.3			13.1–49.3
KLX13A	494.37–494.84	250–500			−5.11	
KLX13A	578.03–578.56	250–500			12.7	−5.11–12.7
KLX13A	494.37–494.84	250–500		42.7		
KLX13A	578.03–578.56	250–500		40.6		40.6–42.7
KLX13A	494.37–494.84	250–500	29			
KLX13A	578.03–578.56	250–500	19.9			19.9–29.0
KLX13A	494.37–494.84	500–1000			9.74	
KLX13A	531.98–532.66	500–1000			52.1	
KLX13A	578.03–578.56	500–1000			−1.25	−1.25–52.1
KLX13A	494.37–494.84	500–1000		35.4		
KLX13A	531.98–532.66	500–1000		106		
KLX13A	578.03–578.56	500–1000		30.7		30.7–106
KLX13A	494.37–494.84	500–1000	23.8			
KLX13A	531.98–532.66	500–1000	47.9			
KLX13A	578.03–578.56	500–1000	16.1			16.1–47.9

Table 4-2. A comparison of measured CEC with different methods on KLX13A at different drill core lengths. Values in green background color are data from sample KLX13A (531.98–532.66 m) which have the highest CEC values.

Drill core	Drill core length (m)	Grain size (µm)	$BaCl_2$ (meq/100 g)	NH_4Ac (meq/100 g)	$Co(NH_3)_6^{3+}$ (meq/100 g)
KLX13A	531.98–532.66	0–63			30.9
KLX13A	494.37–494.84	0–63		68.1	
KLX13A	578.03–578.56	0–63	27.1		
KLX13A	578.03–578.56	63–125			8.90
KLX13A	494.37–494.84	63–125	13.1		
KLX13A	531.98–532.66	63–125	49.3		
KLX13A	494.37–494.84	250–500	29	42.7	3.37
KLX13A	578.03–578.56	250–500	19.9	40.6	17.5
KLX13A	494.37–494.84	500–1000	23.8	35.4	9.74
KLX13A	531.98–532.66	500–1000	47.9	106	52.1
KLX13A	578.03–578.56	500–1000	16.1	30.7	−1.25

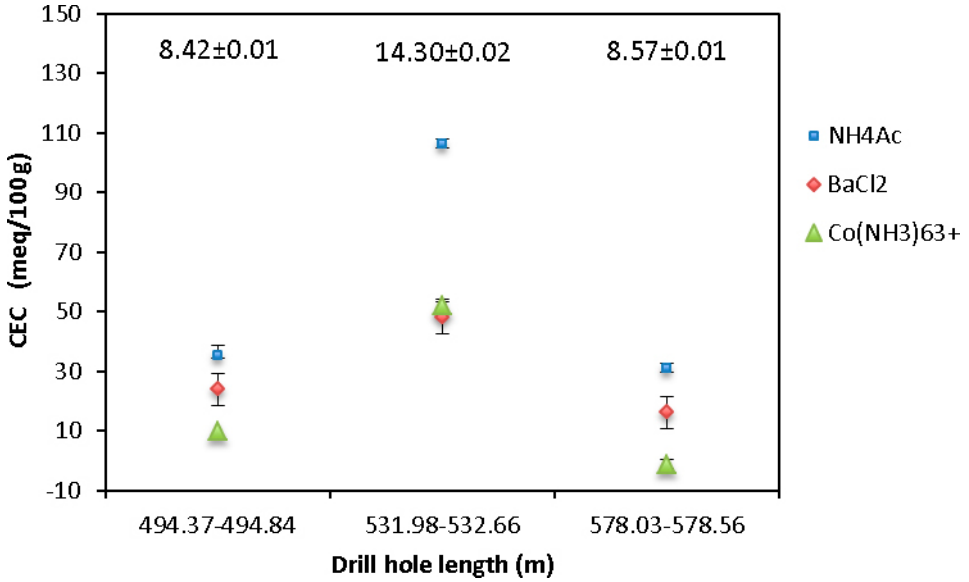

Figure 4-1. *Variation of CEC of KLX13A with depth (m) and where B.E.T. values are indicated in the figure.*

5 Conclusions

It can be concluded that the $Co(NH_3)_6^{3+}$-method is promising when it comes to measuring CEC on samples with a high calcite content because of its inability to dissolve the calcite. The method showed a high consistency among the results and expected grain size dependence. If considering the $Co(NH_3)_6^{3+}$-method to be the most accurate method for analyzing the CEC of fracture coating material in Äspö/Laxemar, the obtained CEC values are up to 52.1 meq/100 g sample.

The $BaCl_2$ method showed CEC values between 13.1 and 53 meq/100 g sample, but these values are likely overestimated due to the dissolution of the calcite in the samples. The method is not recommended for CEC analyses on samples containing calcite.

The NH_4Ac method showed a strong dissolution of calcite and the obtained CEC values were between 30.7 and 170 meq/100 g. This method is also not recommended for CEC analyses on samples containing calcite.

The method in which pure water or aqueous KCl solutions were passed through a sample in a teflon column and in which samples were collected continuously showed unreasonable high CEC values because of the dissolution of both calcite and the other minerals. In a future study the teflon columns could be used with $Co(NH_3)_6^{3+}$ instead of KCl solutions because of the advantage of providing time dependent data on the cation exchange process.

6 Acknowledgements

Carl-Magnus Mörth (Stockholms University), Henrik Drake (Isochron Geoconsulting), Ignasi Puigdomenech (SKB) and Eva-Lena Tullborg (Terralogica AB) are thanked for critical and helpful discussions. Johan Byegård (Geosigma AB) is thanked for his advice regarding experimental methods and performance.

References

SKB's (Svensk Kärnbränslehantering AB) publications can be found at www.skb.com/publications.

Allred B J, Bigham J M, Brown G O, 2007. The impact of clay mineralogy on nitrate mobility under unsaturated flow conditions. Vadose Zone Journal 6, 221–232.

Byegård J, Tullborg E-L, 2012. Äspö Hard Rock Laboratory. Sorption experiments and leaching studies using fault gouge and rim zone material from the Äspö Hard Rock Laboratory. TRUE-1 Continuation project. SKB P-11-20, Svensk Kärnbränslehantering AB.

Carlsten S, Stråhle A, Hultgren P, Mattsson H, Stanfors R, Wahlgren C-H, 2007. Oskarshamn site investigation. Geological single-hole interpretation of KLX13A, HLX39 and HLX41. SKB P-07-156, Svensk Kärnbränslehantering AB.

Dohrmann R, Kaufhold S, 2009. Three new, quick CEC methods for determining the amounts of exchangeable calcium cations in calcareous clays. Clays and Clay Minerals 57, 338–352.

Drever J I, 1973. The preparation of oriented clay mineral specimens for X-ray diffraction analysis by a filter-membrane peel technique. American Mineralogist 58, 553–554.

Farhadi S, Pourzare K, 2012. Simple and low-temperature preparation of Co_3O_4 sphere-like nanoparticles via solid-state thermolysis of the $[Co(NH_3)_6](NO_3)_3$ complex. Materials Research Bulletin 47, 1550–1556.

Faure G, 1998. Principles and applications of geochemistry: a comprehensive textbook for geology students. 2nd ed. Upper Saddle River, NJ: Prentice Hall.

Frogner P, Schweda P, 1998. Hornblende dissolution kinetics at 25°C. Chemical Geology 151, 169–179.

Krauskopf K B, 1979. Introduction to geochemistry. 2nd ed. New York: McGraw-Hill.

Liu C L, Wang M K, Yang C C, 2001. Determination of cation exchange capacity by one-step soil leaching column method. Communications in Soil Science and Plant Analysis 32, 2359–2372.

Ross D S, Ketterings Q, 2011. Recommended methods for determining soil cation exchange capacity. In Recommended soil testing procedures for the Northeastern United States. 3rd ed. University of Delaware. (Northeastern Regional Publication 493)

Ruiz-Agudo E, Kowacz M, Putnis C V, 2010. The role of background electrolytes on the kinetics and mechanism of calcite dissolution. Geochimica et Cosmochimica Acta 74, 1256–1267.

Skinner M F, Zabowski D, Harrison R, Lowe A, Xue D, 2002. Measuring the cation exchange capacity of forest soils. Communications in Soil Science and Plant Analysis 32, 1751–1764.

ISO 11464:2006. Soil quality – Pretreatment of samples for physico-chemical analysis. Geneva: International Organization for Standardization.

ISO 12570:2000. Hygrothermal performance of building materials and products – Determination of moisture content by drying at elevated temperature. International Organization for Standardization.

ISO 13536:1995. Soil quality – Determination of the potential cation exchange capacity and exchangeable cations using barium chloride solution buffered at pH = 8,1. Geneva: International Organization for Standardization.

ISO 23470:2007. Soil quality – Determination of effective cation exchange capacity (CEC) and exchangeable cations using a hexamminecobalt trichloride solution. Geneva: International Organization for Standardization.

Stumm W, Morgan J J, 1981. Aquatic chemistry: an introduction emphasizing chemical equilibria in natural waters. 2nd ed. New York: Wiley.

Sutherland M M J, 1928. The metal-ammines. In Friend J N (ed). A text-book of inorganic chemistry, Vol. X. London: Griffin.

Wahlgren C-H, Curtis P, Hermanson J, Forssberg O, Öhman J, Fox A, La Pointe P, Drake H, Triumf C-A, Mattsson H, Thunehed H, Juhlin C, 2008. Geology Laxemar. Site descriptive modelling, SDM-Site Laxemar. SKB R-08-54, Svensk Kärnbränslehantering AB.

Winberg A (ed), 2010. Fault rock zones characterisation – Final report. TRUE-1 Continuation Project. SKB TR-10-36, Svensk Kärnbränslehantering AB.

Appendix

Table A-1. Elemental compositions of SEM-EDS analyses of KLX09 (represented in Figure 3-2). All values are in wt%.

Element	Wt% Spectrum 1.6.7	±	Wt% Spectrum 3.4.5.12	±	Wt% Spectrum 2.10	±	Wt% Spectrum 8	±	Wt% Spectrum 9	±	Wt% Spectrum 11	±
Fe	44.27	0.23	5.66	1.35	56.07	0.38	3.10	0.31	40.25	4.03	20.99	2.10
O	35.43	2.00	44.36	2.75	20.61	3.95	49.10	4.91	40.36	4.04	35.06	3.51
C	9.80	1.04	10.96	1.23	10.21	1.42	10.40	1.04	9.13	0.91	12.11	1.21
Si	4.50	1.35	19.30	1.13	5.76	1.07	13.50	1.35	4.47	0.45	13.65	1.37
Mg	2.47	0.65	4.52	1.78	2.67	0.37	2.40	0.24	2.05	0.21	6.77	0.68
Al	2.03	0.42	6.88	0.24	2.56	0.36	6.00	0.60	2.13	0.21	5.48	0.55
K	0.97	0.46	7.11	1.81	1.47	0.24	2.00	0.20	1.12	0.11	2.51	0.25
Ca	0.37	0.06	0.87	0.23	0.48	0.11	8.10	0.81	0.32	0.03	1.78	0.18
Ti	0.23	0.06	0.11	0.10	0.20	0.00	5.30	0.53	0.17	0.02	0.48	0.05

Table A-2. Average elemental distribution of the SEM-EDS analyses (spot analyses) of KLX11A represented in Figure 3-4.

(a)			(b)		
Element	**Wt%**	**±**	**Element**	**Wt%**	**±**
O	48.16	0.44	O	50.65	0.265
C	15.99	0.71	Ca	27.62	0.165
Si	10.85	0.13	C	19.16	0.23
Fe	8.66	0.14	Si	0.92	0.03
Mg	7.02	0.10	Fe	0.655	0.055
Al	6.24	0.09	Al	0.47	0.03
Ca	1.64	0.04	Mg	0.43	0.04
K	0.71	0.03			
Mn	0.26	0.04			
(c)			**(d)**		
Element	**Wt%**	**±**	**Element**	**Wt%**	**±**
O	37.84	0.40	O	34.65	0.37
Ca	29.78	0.27	Sn	20.04	0.27
P	13.19	0.14	C	15.82	0.59
C	11.84	0.59	Pb	14.07	0.27
F	2.68	0.22	Si	5.62	0.08
Mg	2.25	0.12	Fe	2.83	0.09
Si	1.69	0.04	Al	2.13	0.06
Fe	1.02	0.07	Mg	2.11	0.06
Al	0.81	0.04	Ca	0.89	0.09
K	0.36	0.03	S	0.66	0.07
Na	0.15	0.04	Cu	0.6	0.1
			K	0.57	0.07

Table A-3. Elemental distribution of the SEM-EDS analyses (spot analyses) of KLX13A (494) represented in Figure 3-6. Similar spectra are averaged.

Spectrum 1–2			Spectrum 3			Spectrum 4–5		
Element	**Average wt%**	**±**	**Element**	**Average wt%**	**±**	**Element**	**Average wt%**	**±**
O	45.08	0.26	O	31.80	0.24	O	42.75	0.27
Na	1.13	0.07	Na	0.57	0.08	Na	0.38	0.06
Mg	4.70	0.09	Mg	4.88	0.09	Mg	5.48	0.09
Al	7.08	0.09	Al	6.10	0.09	Al	7.04	0.09
Si	15.17	0.13	Si	10.45	0.11	Si	13.92	0.13
K	7.82	0.09	K	2.37	0.06	K	5.90	0.09
Ca	0.95	0.06	Ca	1.55	0.05	Ca	1.22	0.06
Ti	0.40	0.07	Ti	1.18	0.06	Ti	0.40	0.06
Mn	0.39	0.08	Mn	0.83	0.10	Mn	0.39	0.09
Fe	16.69	0.19	Fe	39.35	0.24	Fe	22.02	0.21
			Cu	0.64	0.16			
			Mo	0.28	0.08			

Table A-4. Elemental distribution of the SEM-EDS analyses (spot analyses) of KLX13A (531) represented in Figure 3-8. The unreasonably high C content is due to the influence from the carbon tape on which the samples are mounted.

(a)			(b)		
Element	**Wt%**	**±**	**Element**	**Wt%**	**±**
C	32.66	0.54	C	24.70	0.75
O	34.95	0.34	O	35.90	0.43
Na	0.25	0.03	Na	0.18	0.04
Mg	4.94	0.07	Mg	0.43	0.04
Al	3.45	0.06	Al	1.91	0.05
Si	6.10	0.07	Si	11.47	0.14
S	0.30	0.02	K	2.19	0.05
K	0.23	0.02	Fe	0.51	0.06
Ca	0.45	0.03	Zr	22.58	0.30
Ti	0.26	0.03	Ca	0.12	0.03
Mn	0.39	0.05			
Fe	16.17	0.18			
(c)			**(d)**		
Element	**Wt%**	**±**	**Element**	**Wt%**	**±**
C	35.10	0.53	C	28.19	0.23
O	9.51	0.23	O	48.78	0.25
Mg	0.45	0.04	Mg	0.40	0.03
Al	0.38	0.03	Al	0.27	0.03
Si	0.83	0.04	Si	0.52	0.03
Ca	0.22	0.03	S	0.06	0.02
Fe	25.56	0.26	Ca	21.56	0.13
			Fe	0.26	0.04

Table A-5. Elemental distribution of the SEM-EDS analyses (spot analyses) of KLX13A (578) represented in Figure 3-10. The unreasonably high C content is due to the influence from the carbon tape on which the samples are mounted.

(a)			(c) (Grey areas)		
Elements	**Wt%**	**±**	**Elements**	**Wt%**	**±**
C	33.91	0.29	C	41.50	0.44
O	36.91	0.24	O	35.48	0.32
Mg	4.81	0.06	Na	0.00	0.00
Al	4.16	0.06	Mg	2.62	0.04
Si	5.87	0.06	Al	3.70	0.05
S	0.10	0.02	Si	8.00	0.09
Mn	0.28	0.04	S	0.06	0.02
Fe	13.84	0.13	K	2.43	0.04
			Ca	0.48	0.03
			Cr	0.00	0.00
			Mn	0.15	0.03
			Fe	5.30	0.09
			Ni	0.00	0.00
(b)			**(c) (White area)**		
Elements	**Wt%**	**±**	**Elements**	**Wt%**	**±**
C	37.13	0.35	C	42.27	0.40
O	28.32	0.29	O	17.07	0.20
Na	0.22	0.04	Na	0.21	0.03
Mg	0.36	0.03	Mg	1.43	0.04
Al	3.28	0.05	Al	1.75	0.04
Si	7.99	0.08	Si	3.06	0.04
S	0.13	0.02	S	0.27	0.02
Cl	0.18	0.03	K	0.17	0.02
Ca	5.32	0.07	Ca	0.61	0.03
Ti	0.85	0.06	Cr	5.19	0.07
Mn	0.34	0.06	Mn	0.74	0.05
Fe	6.17	0.11	Fe	23.32	0.20
La	4.09	0.19	Ni	3.90	0.09
Ce	4.85	0.16			
Nd	0.63	0.15			

Table A-6. Concentrations of released Ca, Na, Mg, Al, Mn and Fe into solution using flow-through leaching experiments on KLX09 (720.15–720.30 m), grain size 0–125 µm, with 0.001 M KCl solution.

KLX09 Time (min)	**Ca (ppb)**	**Na (ppb)**	**Mg (ppb)**	**Al (ppb)**	**Mn (ppb)**	**Fe (ppb)**	**K (ppb)**
20	45240	1407	5402	273	98.2	471	44050
40	14985	170200	2245	437	48.1	689	43820
60	15125	78516	2141	320	38.7	428	38190
80	13063	33515	1820	212	32.2	262	28620
100	10923	14080	1488	146	29.1	238	22750
120	8972	8369	1183	164	23.9	213	17840
140	7235	4483	1093	192	22.7	268	13710
160	7039	−104.8	1065	178	23.8	319	11960
190	6873	491.5	979	30.5	24.5	82.1	14020
210	4242	−285.3	662	184	23.2	137	8835
230	4392	795.3	649	56.7	24.2	87.7	7665
250	3541	−3735	478	46.3	17.7	61.6	10570
Sum (mg/L)	142	311.8	19.2	2.24	0.41	3.26	262

Table A-7. Concentrations of released Ca, Na, Mg, Al, Mn and Fe into solution using flow-through leaching experiments on KLX09 (720.15–720.30 m), grain size 0–125 µm, with 0.01 M KCl solution.

KLX09 Time (min)	Ca (ppb)	Na (ppb)	Mg (ppb)	Al (ppb)	Mn (ppb)	Fe (ppb)	K (ppb)
20	0	7497	8544	44.6	164	92.5	81370
40	39650	3606	4445	38.8	95.5	119	56540
60	26885	1371	2810	51.9	67.7	118	41510
80	22545	1049	2339	52.0	60.2	111	39030
100	18990	528	1981	46.9	50.8	104	30900
120	15650	681	1547	48.7	45.5	101	25610
140	12493	462	1228	52.0	38.2	113	24650
170	12277	347	1236	57.2	38.0	121	26080
200	8667	43.5	783	66.5	32.2	157	23450
230	7371	−45.3	790	85.6	29.8	129	9906
260	6967	411	674	86.1	29.1	188	5763
290	5943	248	577	61.0	25.3	159	6496
320	5828	406	698	188	29.8	368	3604
Sum (mg/L)	183.3	16.65	27.65	0.88	0.71	1.88	374.9

Table A-8. Concentrations of released Ca, Na, Mg, Al, Mn and Fe into solution using flow-through leaching experiments on KLX09 (720.15–720.30 m), grain size 0–125 µm, with 0.02 M KCl solution.

KLX09 Time (min)	Ca (ppb)	Na (ppb)	Mg (ppb)	Al (ppb)	Mn (ppb)	Fe (ppb)	K (ppb)
20	8936	450	575	−6.74	53.3	11.1	15480
40	9874	297	729	8.83	50.6	11.2	12420
60	10108	280	637	−7.68	46.8	17.1	15300
80	9825	514	698	−13.2	44.6	25.1	13480
100	9237	172	800	154	44.5	350	7328
120	8568	248	674	86.6	41.1	246	13100
140	7922	136	594	93.5	39.6	286	15490
170	6793	154	513	67.7	33.3	152	15160
200	6422	164	507	75.1	33.2	189	8362
230	5859	206	424	44.0	28.8	116	12800
260	5184	218	299	46.1	28.0	101	13660
290	4902	377	251	5.05	24.9	77.6	10960
320	4645	−4.9	302	60.1	25.9	102	11930
350	4177	314	217	40.2	24.1	84.4	12660
Sum (mg/L)	102.5	3.53	7.22	0.65	0.52	1.77	178.1

Table A-9. Concentrations of released Ca, Na, Mg, Al, Mn and Fe into solution using flow-through leaching experiments on KLX13A (494.37–494.84 m), grain size 0–125 µm, with deionized water.

KLX13A Time (min)	Ca (ppb)	Na (ppb)	Mg (ppb)	Al (ppb)	Mn (ppb)	Fe (ppb)	K (ppb)
20	29060	12290	4786	35.1	48.2	2.43	2799
40	26730	12380	4382	35.2	39.0	2.73	2728
60	26870	12100	4390	41.2	37.6	5.50	2792
80	26590	11920	4321	37.6	33.9	3.71	2810
100	26470	11900	4302	35.7	32.1	5.63	2792
120	26580	11800	4325	32.4	29.6	6.95	2865
140	26440	11970	4301	34.7	27.9	8.02	2821
160	26670	11850	4338	40.7	31.6	5.18	2774
180	26560	11830	4326	35.9	33.0	6.66	2775
200	26660	11820	4347	37.9	32.7	5.91	2793
220	26870	11970	4360	40.7	32.7	5.17	2804
240	26530	11810	4321	39.3	31.2	7.47	2801
Sum (mg/L)	322.0	143.6	52.5	0.45	0.41	0.07	33.6

Table A-10. Concentrations of released Ca, Na, Mg, Al, Mn and Fe into solution using flow-through leaching experiments on KLX13A (578.03–578.56 m), grain size 0–125 µm, with deionized water.

KLX13A Time (min)	Ca (ppb)	Na (ppb)	Mg (ppb)	Al (ppb)	Mn (ppb)	Fe (ppb)	K (ppb)
20	30090	32560	5629	83.9	58.6	58.8	4256
40	37620	74570	7869	53.6	75.5	9.26	5157
60	26680	45800	5768	55.8	51.8	5.02	4207
80	22030	26650	4773	57.2	48.5	11.04	3338
100	22640	21560	4902	61.4	62.9	20.1	3144
120	22200	27340	4775	60.7	53.3	22.3	3314
140	20840	24020	4434	77.3	49.6	45.4	3106
160	21650	17920	4578	50.7	61.0	17.2	2931
180	22700	16990	4700	49.7	69.5	20.6	2863
200	22550	16850	4714	55.0	74.5	25.3	2847
220	22780	17260	4701	56.6	78.8	32.0	3371
240	22880	16770	4688	44.7	77.9	17.6	2818
260	23310	16560	4705	51.0	73.1	22.6	2895
280	24280	16260	4807	47.2	71.3	23.1	2977
Sum (mg/L)	342.3	371.1	71.0	0.80	0.91	0.33	47.2

Table A-11. Concentrations of released Ca, Na, Mg, Al, Mn and Fe into solution using flow-through leaching experiments on KLX13A (494.37–494.84 m), grain size 125–250 µm, with deionized water.

KLX13A Time (min)	Ca (ppb)	Na (ppb)	Mg (ppb)	Al (ppb)	Mn (ppb)	Fe (ppb)	K (ppb)
10	11810	4870	4202	2623	138	6462	869
20	7945	2623	3713	2723	127	6356	508
40	6031	1571	2498	1908	83.0		330
50	5315	1207	1447	1009	43.6	2382	235
60	5081	758	1088	710	31.1	1678	187
70	4546	526	920	600	24.5	1272	162
80	4413	445	695	424	16.9	931	122
90	3994	309	706	509	20.4	1114	113
100	4079	194	662	507	18.3	1093	96.4
110	4025	239	609	457	15.4	881	92.9
120	3744	127	429	311	9.3	565	67.6
Sum (mg/L)	60983	12867	16969	11780	527	22733	2783

Table A-12. Concentrations of released Ca, Na, Mg, Al, Mn and Fe into solution using flow-through leaching experiments on KLX13A (578.03–578.56 m), grain size 125–250 µm, with deionized water.

KLX13A Time (min)	Ca (ppb)	Na (ppb)	Mg (ppb)	Al (ppb)	Mn (ppb)	Fe (ppb)	K (ppb)
10	8571	7237	4004	2950	213	6651	1136
20	5253	4480	4444	3858	242	8930	765
40	3525	2757	3065	2689	157	5881	669
50	2796	1956	2164	1899	111	4099	632
60	2118	1337	1439	1260	72.6	2591	562
70	1595	765	1150	1069	58.2	2176	507
80	1334	393	872	826	45.3	1657	447
90	1181	335	866	802	42.5	1603	408
100	1008	164	780	766	40.8	1587	359
110	937	226	681	672	33.7	1336	328
120	868	32.7	527	521	26.6	1000	279
Sum (mg/L)	29187	19683	19992	17312	1043	37511	6091

Table A-13. Concentrations of released Ca, Na, Mg, Al, Mn and Fe into solution using flow-through leaching experiments on KLX16A (33.95–34.20 m) , grain size 0–125 µm, with 0.001 M KCl solution.

KLX16A Time (min)	Ca (ppb)	Na (ppb)	Mg (ppb)	Al (ppb)	Mn (ppb)	Fe (ppb)	K (ppb)
20	3470	380	490	34.5	16.0	37.3	9268
40	46490	13610	6125	125	64.6	165	28100
60	28740	7907	3627	172	42.5	127	17610
80	17890	4039	2168	228	28.6	122	12200
100	12510	1799	1401	258	21.1	122	8521
120	9392	1349	1087	277	16.2	133	6019
140	8069	940	853	277	16.0	118	5781
160	6997	594	720	244	13.0	90.2	6036
190	6513	624	584	243	12.9	66.2	5358
210	7883	1557	878	233	21.1	223	4864
230	4631	528	408	141	11.4	42.5	13180
250	5048	318	398	164	10.8	35.2	5424
Sum (mg/L)	157.6	31.2	18.74	2.40	0.27	1.28	122.4

Table A-14. Concentrations of released Ca, Na, Mg, Al, Mn and Fe into solution using flow-through leaching experiments on KLX16A (33.95–34.20 m) , grain size 0–125 µm, with 0.01 M KCl solution.

KLX16A Time (min)	Ca (ppb)	Na (ppb)	Mg (ppb)	Al (ppb)	Mn (ppb)	Fe (ppb)	K (ppb)
20	53000	475	2561	96.4	104	104	29360
40	26860	154	1204	135	50.3	136	12830
60	21230	200	835	148	38.7	109	14480
80	27080	323	1236	171	53.2	208	10850
100	14157	285	545	266	32.1	392	3805
120	9208	−82.0	423	265	23.4	365	635
140	8307	98.2	223	195	18.6	186	2506
160	8323	179	190	160	16.0	173	−3564
190	7743	286	144	175	18.1	216	1237
210	7327	9.43	223	150	15.9	154	2060
230	7436	216	201	173	16.7	172	4751
250	7052	391	100	111	13.3	104	3489
Sum (mg/L)	197.7	1.95	7.89	2.05	0.40	2.32	82.4

Table A-15. Concentrations of released Ca, Na, Mg, Al, Mn and Fe into solution using flow-through leaching experiments on KLX16A (33.95–34.20 m) , grain size 0–125 µm, with 0.02 M KCl solution.

KLX16A Time (min)	Ca (ppb)	Na (ppb)	Mg (ppb)	Al (ppb)	Mn (ppb)	Fe (ppb)	K (ppb)
20	19940	318	194	62.8	22.0	21.5	27530
40	16560	−1.49	163	157	19.0	258	20530
60	11427	102	130	165	14.5	200	14820
80	9435	27.5	44.8	145	12.3	97.9	12020
100	8565	272	50.3	125	11.2	88.0	11450
120	7887	222	134	96.9	11.3	73.1	15350
140	7746	171	125	97.8	10.6	61.7	10340
160	7493	258	−7.51	61.7	10.5	65.4	9890
190	7355	220	92.23	87.9	11.6	50.9	14930
210	7176	275	30.21	95.1	12.2	81.8	20110
230	7244	328	103	69.7	9.81	48.6	10990
250	7432	250	78.7	65.2	10.4	28.9	8989
Sum (mg/L)	118.3	1.66	1.14	1.23	0.16	1.08	177.0

Table A-16. Concentrations of released Ca, Na, Mg, Al, Mn and Fe into solution using the $BaCl_2$-method.

Drill core	Drill core length (m)	Grain size (µm)	Al (ppm)	Ca (ppm)	Fe (ppm)	K (ppm)	Mg (ppm)	Mn (ppm)	Na (ppm)
Blank			0.054	0.992	0.021	0.416	0.132	0.020	0.980
KA1596A02	4.32–5.00	0–63	0.266	185	1.733	3.080	6.0	0.509	5.310
KLX13A	578.03–578.56	0–63	0.747	121	5.434	1.470	14.8	1.410	5.250
KLX09	720.15–720.30	0–63	0.193	63.9	1.001	0.963	5.177	0.344	2.880
KLX13A	494.37–494.84	63–125	0.321	142	4.490	2.220	17.2	0.503	5.470
KLX13A	531.98–532.66	63–125	0.266	92.8	1.508	0.991	6.21	0.509	5.190

Table A-17. Concentrations of released Ca, Na, Mg, Al, Mn and Fe into solution using the NH_4Ac-method.

Drill core	Drill core length (m)	Grain size (µm)	Mass (g)	Al (ppm)	Ca (ppm)	Fe (ppm)	K (ppm)	Mg (ppm)	Mn (ppm)	Na (ppm)
Blank			0	0.013	0.652	0.0123	0.089	0.837	0.004	0.525
KA1596A02	4.32–5.00	63–125	4.361	0.052	275.9	0.0998	1.837	5.772	1.979	37.26
KLX08	218.54–218.75	63–125	3.765	0.178	111.3	0.142	4.351	7.961	1.344	8.995
KLX13A	494.37–494.84	0–63	4.588	0.099	225	0.198	1.871	8.894	1.359	16.68
KLX09	720.15–720.30	63–125	1.06	0.106	98.78	0.14	1.474	8.665	0.785	23.71
KLX11A	510.45–510.67	0–63	2.068	0.088	254.1	0.0998	2.082	8.289	1.007	21.4

Table A-18. Concentrations of Cobalt and CEC from the $Co(NH_3)_6^{3+}$-method. The difference in Co-concentrations (initial-sample) is denoted "q", while "V" denotes the sample volume (50 mL in this case), and "m" is the sample mass.

Sample name	Drill core length (m)	Sample grain size (µm)	Sample mass (g)	Co (mol/L)	Uncertainty 5 %	*q* (initial-sample)	*q* uncertainty	CEC (300 *q V*) /*m*
Blank			0	1.56×10^{-2}	7.81×10^{-4}	9.74×10^{-4}	8.30×10^{-4}	14.6
KLX08	218.54–218.75	0–63	4.1102	1.49×10^{-2}	7.47×10^{-4}	1.67×10^{-3}	1.58×10^{-3}	6.1
KLX16A	33.95–34.20	0–63	4.2335	1.58×10^{-2}	7.89×10^{04}	8.11×10^{-4}	1.62×10^{-3}	2.9
KLX13A	531.98–532.66	0–63	1.6719	1.32×10^{-2}	6.58×10^{-4}	3.45×10^{-3}	1.49×10^{-3}	30.9
KLX16A	33.95–34.20	63–125	2.4581	1.63×10^{-2}	8.17×10^{-4}	2.66×10^{-4}	1.65×10^{-3}	1.6
KLX11A	510.45–510.67	63–125	1.3489	1.56×10^{-2}	7.79×10^{-4}	1.02×10^{-3}	1.61×10^{-3}	11.3
KLX13A	578.03–578.56	63–125	6.9874	1.25×10^{-2}	6.23×10^{-4}	4.15×10^{-3}	1.45×10^{-3}	8.9
Blank			0	1.97×10^{-2}	9.87×10^{-4}	-3.13×10^{-3}	1.82×10^{-3}	−47.0
KLX13A	494.37–494.84	250–500	5.0194	1.83×10^{-2}	9.15×10^{-4}	-1.71×10^{-3}	1.75×10^{-3}	−5.1
KLX13A	578.03–578.56	250–500	5.0040	1.24×10^{-2}	6.18×10^{-4}	4.24×10^{-3}	1.45×10^{-3}	12.7
KLX13A	494.37–494.84	500–1000	5.0121	1.33×10^{-2}	6.67×10^{-4}	3.25×10^{-3}	1.50×10^{-3}	9.7
KLX13A	531.98–532.66	500–1000	5.0212	-8.26×10^{-4}	-4.13×10^{-5}	1.74×10^{-2}	7.89×10^{-4}	52.1
KLX13A	578.03–578.56	500–1000	5.0244	1.70×10^{-2}	8.51×10^{-4}	-4.19×10^{-4}	1.68×10^{-3}	−1.3